


12-2015

# Sustainability Assessment for Energy Systems and Chemical Process Industries

Michael J. Matzen

*University of Nebraska-Lincoln*, [mmatzen1@gmail.com](mailto:mmatzen1@gmail.com)

Follow this and additional works at: <http://digitalcommons.unl.edu/chemengtheses>

 Part of the [Chemical Engineering Commons](#), and the [Environmental Engineering Commons](#)

---

Matzen, Michael J., "Sustainability Assessment for Energy Systems and Chemical Process Industries" (2015). *Chemical & Biomolecular Engineering Theses, Dissertations, & Student Research*. 27.  
<http://digitalcommons.unl.edu/chemengtheses/27>

This Article is brought to you for free and open access by the Chemical and Biomolecular Engineering, Department of at DigitalCommons@University of Nebraska - Lincoln. It has been accepted for inclusion in Chemical & Biomolecular Engineering Theses, Dissertations, & Student Research by an authorized administrator of DigitalCommons@University of Nebraska - Lincoln.

SUSTAINABILITY ASSESSMENT FOR ENERGY SYSTEMS AND CHEMICAL  
PROCESS INDUSTRIES

by

Michael Joseph Matzen

A THESIS

Presented to the Faculty of  
The Graduate College at the University of Nebraska  
In Partial Fulfillment of Requirements  
for the Degree of Master of Science.

Major: Chemical Engineering

Under the Supervision of Professor Yaşar Demirel

Lincoln, Nebraska

December, 2015

# SUSTAINABILITY ASSESSMENT FOR ENERGY SYSTEMS AND CHEMICAL PROCESS INDUSTRIES

Michael Joseph Matzen, M.S.

University of Nebraska, 2015

Advisor: Yaşar Demirel

Sustainability has become an important factor in the chemical process and energy industries with a strong drive for process improvements towards more environmentally conscious solutions. However, there are many ways of defining sustainability and even more ways of trying to determine how sustainable a process is. This work looks into applying a conjunction of tools including; process simulation, multi-criteria decision matrices and life-cycle assessment to more quantitatively determine sustainability metrics. We have applied these tools for the production of electricity, methanol and dimethyl ether. A novel method of electricity production, in chemical looping combustion (CLC), was used that inherently involves carbon dioxide capture. Experimental work was conducted for two different oxygen carriers,  $\text{CaSO}_4$  and  $\text{CuO}$ , using thermogravimetric analysis (TGA). Process simulations were developed for both coal and natural gas (NG) feedstocks to produce power and heat. Sustainability metrics were developed based on simulated data showing electricity prices of 23.7 ¢/kWhr (NG) and 7.8 ¢/kWhr (coal) while reducing  $\text{CO}_2$  emissions 0.38 (NG) and 3.38 (coal) metric ton/MWhr electricity. Renewable methanol production was also simulated in Aspen Plus. This process used wind based electrolytic hydrogen and captured  $\text{CO}_2$  as feedstocks. This work presents a multi-criteria decision matrix for the inclusion of sustainability metrics

alongside economic indicators in feasibility analysis. A comparison of renewable methanol to NG based methanol using this matrix shows that the renewable process is feasible. We continued this work to conduct a full (cradle-to-grave) life-cycle assessment of alternative fuels based on this renewable methanol and its conversion to dimethyl ether. Using renewable methanol as a fuel reduces greenhouse gas emissions 86% and fossil fuel use by 91% compared to conventional gasoline. Using dimethyl ether reduces greenhouse gas emissions 80% and fossil fuel use 81% when compared to ultra-low sulfur diesel. This whole work focuses on developing sustainability metrics helps identify a quantified measure of sustainability that can be used along economic indicators in a multi-criteria decision matrix for a better and comprehensive feasibility evaluation of energy systems and chemical processes.

## **Dedication**

I would like to first like to thank the Chemical and Biomolecular Engineering Department at the University of Nebraska – Lincoln. The work and effort they have put in the last six and a half years towards my education has been invaluable. I would especially like to thank my advisor, Dr. Yaşar Demirel. Without him this work would not have been possible and his constant advice as a mentor for me in my graduate work is greatly appreciated.

I would also like to thank my family for their help outside of the classroom. My parents provided the opportunities for me at an early age to explore my creativity and expand my knowledge and pursue my love for science. I like to think fostered my ability to achieve at the level I am at. I would also like to thank my wonderful fiancée Jessica Pinkerton and our son Dominic. They were the main motivation for this work and a constant reminder of what I did this for.

Finally I would like to thank God for the grace and blessings I have been given in life. Through Him all things are possible.

## **Grant Information**

I would like to acknowledge the Electric Power Research Institute (EPRI) for providing the grant that funded the majority of the chemical looping combustion work I completed.

Without their support this work would not have been done. I would also like to acknowledge the support Nebraska Public Power District provided in the past which provided a start in the methanol work I completed.

## Table of Contents

CHAPTER 1 INTRODUCTION .....	1
CHAPTER 2 SUSTAINABILITY .....	3
2.1 Sustainability Metrics.....	3
2.2 Life-Cycle Assessment.....	4
CHAPTER 3 ENERGY SYSTEMS .....	8
3.1 Chemical Looping Combustion .....	8
3.2 Materials and Methods.....	12
3.3 Discussion .....	16
3.3.1 CuO Trials.....	16
3.3.2 CaSO <sub>4</sub> Trials .....	18
3.4 CLC Simulations .....	20
3.4.1 Coal CLC plant .....	21
3.4.2 LNG CLC plant.....	23
3.5 Sustainability Metrics of the CLC plants .....	24
3.6 Conclusions .....	26
CHAPTER 4 CHEMICAL PROCESS INDUSTRIES - METHANOL.....	28
4.1 Introduction .....	28
4.2 Conventional Methanol Production .....	33
4.2.1 Syngas Production .....	33

4.2.2	Methanol Conversion.....	34
4.2.3	Methanol Purification .....	35
4.3	Green Production.....	36
4.3.1	H <sub>2</sub> Production.....	37
4.3.2	CO <sub>2</sub> Production.....	38
4.3.3	Methanol from CO <sub>2</sub> and H <sub>2</sub> .....	39
4.4	Materials and Methods .....	39
4.5	Results .....	44
4.5.1	Sustainability.....	44
4.5.2	Economic Analysis .....	48
4.5.3	Multi-Criteria Decision Matrix.....	51
4.6	Conclusions .....	53
CHAPTER 5 CHEMICAL PROCESS INDUSTRIES – DIMETHYL ETHER.....		55
5.1	Introduction .....	55
5.2	Materials and Methods .....	58
5.2.1	Dimethyl Ether Simulation .....	58
5.2.2	Life-Cycle Assessment .....	63
5.3	Results and Analysis .....	71
5.3.1	Cradle-to-Gate Analysis.....	71
5.3.2	Cradle-to-Grave Analysis .....	75



5.4	Conclusions .....	77
CHAPTER 6 CONCLUSIONS, RECOMMENDATIONS AND FUTURE WORK .....		79
APPENDIX A: CHEMICAL LOOPING COMBUSTION .....		81
APPENDIX B: METHANOL PRODUCTION .....		87
APPENDIX C: LIFE-CYCLE ASSESSMENT .....		90
PUBLICATIONS LIST (RELEVANT TO THESIS).....		92
REFERENCES .....		<b>Error! Bookmark not defined.</b>

## List of Figures

Figure 3.1: Predicted atmospheric CO <sub>2</sub> concentrations compared to emissions	8
Figure 3.2: A diagram outlining the process of chemical looping combustion for power production with carbon capture in a fixed bed system (a) and a circulating fluidized bed system (b)	10
Figure 3.3: Experimental data showing the mass loss and CO <sub>2</sub> emissions for a CuO/coal sample	16
Figure 3.4: Experimental data showing the mass loss and CO <sub>2</sub> emissions for a CaSO <sub>4</sub> /coal sample	18
Figure 3.5: A comparison between the CaSO <sub>4</sub> blank and a CaSO <sub>4</sub> and coal sample showing mass loss attributed to water evaporation	19
Figure 3.6: Process flow diagram of the coal based CLC plant; streams in bold represent inputs and outputs	21
Figure 3.7: A LNG based CLC cogeneration plant where again bolded streams are inputs and outputs	24
Figure 4.1: Methanol price and demand in recent history	30
Figure 4.2: World methanol demand according to use	31
Figure 4.3: A flow diagram presenting the ICI low pressure methanol synthesis	36
Figure 4.4: Process flow diagram of the methanol plant using a Lurgi reactor and producing steam	40
Figure 4.5: Some economic and sustainability indicators in the integral methanol production facility	45
Figure 4.6: Overall energy balance for the integral methanol production facility	46

Figure 4.7: The influence of H <sub>2</sub> production cost on: (a) net present value at constant methanol (MeOH) price, (b) Selling price of methanol for NPV = 0 with and without selling O <sub>2</sub> byproduct at \$100/mt	50
Figure 5.1: Process flow diagram for the backend DME facility	59
Figure 5.2: A map detailing the system boundary of the LCA and the inputs/outputs and processes we are investigating.	62
Figure 5.3: Emissions and energy use for methanol production divided by each section of the process	72
Figure 5.4: Emissions and energy use for dimethyl ether production divided by each section of the process	72
Figure 5.5: Normalized midpoint indicators for both DME and methanol production processes. Impacts from individual process sections are shown as different textures	74
Figure 5.6: Cradle-to-grave emissions for methanol and dimethyl ether; shown for comparison are emissions from biomass gasification based methanol and DME, natural gas based methanol and DME, gasoline, ultra-low sulfur diesel and liquefied natural gas	76

## List of Tables

Table 3.1: The TGA schedule ran for all of the TGA tests	12
Table 3.2: Proximate and ultimate analysis for the coal sample used	13
Table 3.3: Results of the reduction phase of the chemical looping trials	15
Table 3.4: Results for the reoxidation section of the chemical looping trials	16
Table 3.5: Sustainability metrics for the CLC simulations using coal and natural gas	26
Table 4.1: Column specifications and results for column T101	43
Table 4.2: Sustainability indicators for the integral methanol plant	46
Table 4.3: Sustainability metrics for the integral methanol plant, with steam production (a) and with steam utilization (b)	47
Table 4.4: Effect of methanol selling price on the maximum unit production cost of renewable hydrogen (NPV = 0 after 10 years).	51
Table 4.5: Multi-criteria decision matrix for feasibility assessment of chemical processes and energy systems.	53
Table 5.1: Operating conditions and results for the three heat exchangers	60
Table 5.2: Column specifications and results for the DME process towers	61
Table 5.3: Unit energy cost for various utilities with energy source of natural gas for 2014	67
Table 5.4: Comparative indicators for methanol and dimethyl ether facilities	74
Table 5.5: Non-normalized environmental impacts for mt of product (methanol or dimethyl ether)	75

## List of Equations

1: Combustion reaction in CLC	9
2: Reoxidation reaction of metal oxide in CLC	10
3: Combustion of coal with $\text{CaSO}_4$ metal oxide	13
4: Combustion of coal with $\text{CuO}$ metal oxide	13
5: Volume calculation for $\text{CO}_2$ emitted during TGA experiments	14
6: Mass calculation for $\text{CO}_2$ emitted during TGA experiments	14
7: % conversion calculation for TGA experiments	14
8: Theoretical $\text{CO}_2$ emissions for a coal sample	15
9: Reoxidation of $\text{CaS}$ with oxygen	15
10: Reoxidation of $\text{Cu}$ with oxygen	15
11: % reoxidation calculation for TGA experiments	15
12: Thermal decomposition of $\text{CuO}$ releasing $\text{O}_2$	17
13: Thermal decomposition of $\text{CaSO}_4$ releasing $\text{SO}_2$ and $\text{O}_2$	19
14: Solid-solid decomposition of $\text{CaSO}_4$ and $\text{CaS}$	20
15: Partial oxidation reaction of carbon in coal	33
16: Steam reforming reaction of carbon in coal	33
17: Steam reforming reaction of methane (natural gas)	33
18: Partial oxidation reaction of methane (natural gas)	33
19: Dry reforming reaction of methanol (natural gas)	33
20: Water gas shift reaction	34
22: $\text{CO}_2$ hydrogenation to methanol	35
23: Water splitting reaction during electrolysis	35

23: Water splitting reaction during electrolysis	37
24: Sugar fermentation to ethanol and CO <sub>2</sub>	39
25: Ergun equation for pressure drop in the methanol reactor	41
26: Rate equation for CO hydrogenation	42
27: Rate equation for CO <sub>2</sub> hydrogenation	42
28: Cost estimation update based on CEPCI	48
29: Equation for economic constraint	48
30: Equation for unit product cost	49
31: Methanol dehydration to dimethyl ether	55
32: Equation for fossil fuel energy ratio	73
33: Equation for life cycle efficiency	73
34: Equation for carbon fixation fraction	73

## CHAPTER 1 INTRODUCTION

The majority of this work deals in determining the sustainability of processes using quantifiable methods. The need for quantification stems from a desire to comparatively analyze different processes. This is done to ultimately make some decision that benefits the overall sustainability of our actions on this planet. We focus on the tools able to quantify and compare sustainable processes including; process modeling for determination of sustainability metrics, multi-criteria decision matrices for inclusion of economic and sustainability metrics in feasibility analyses, and life-cycle assessment for the quantification of the total cradle-to-grave environmental burdens of a product. We apply these tools to both energy systems and chemical process industries. Processes including chemical looping combustion, renewable methanol and dimethyl ether are addressed.

Chemical looping combustion (CLC) is a novel method of energy production that inherently includes carbon capture. We produced Aspen Plus simulations for CLC using coal and natural gas as fuels. These simulations develop some process specifications for CLC and determine the feasibility of these processes. Electricity is able to be produced with a utilities cost of 7.8¢/kWhr (coal) and 23.7 ¢/kWhr (natural gas) while only emitting 0.90 (coal) and 1.06 (natural gas) mt of CO<sub>2</sub> equivalents per MWhr produced. We also have produced experimental results, using thermogravimetric analysis, for two different metal oxide oxygen carriers, CaSO<sub>4</sub> and CuO, for the chemical looping combustion of coal. These tests show potential high coal conversions (95 - 97%) and reoxidation percentages of 80-81%.

We also produced an Aspen Plus simulation of a renewable methanol production facility. In this work methanol is produced from wind-based electrolytic hydrogen and CO<sub>2</sub> captured and compressed from a bioethanol facility. Hydrogen production cost was shown to be the critical economic variable and costs were determined to range from \$0.40 to \$0.70/kg of H<sub>2</sub> for economic feasibility. However the sustainability of this process was addressed and compared to conventional (natural gas-based) methanol production. A comparison using a novel multi-criteria decision matrix showed that renewable methanol may be more feasible if sustainability indicators are included in the feasibility analysis. This matrix was also used to compare renewable ammonia to fossil-based ammonia to highlight its use for fuels, energy and chemical feedstock production. We also investigated the sustainability of using this renewable methanol as a transportation fuel using a life-cycle assessment (LCA). In this work we included the potential conversion of methanol into dimethyl ether. LCA includes the total environmental impact a product has from the production of its raw materials to its eventual use and disposal. We compare our renewable methanol and dimethyl ether to conventional natural gas based methanol and dimethyl ether production and its use as a fuel to conventional petroleum fuels (diesel, gasoline and liquefied natural gas). Our renewable method was shown to lower life-cycle greenhouse gas emissions by 82-86%, minimize other criteria pollutant emissions and reduce fossil fuel depletion by 82-91%, when compared to petroleum fuels. Collectively these works present a substantial review into the use of readily available tools for the quantification of sustainability in both the energy sector and chemical process industries.



## CHAPTER 2 SUSTAINABILITY

### 2.1 Sustainability Metrics

Sustainability is a concern in many industrial and academic circles. There is a clear drive for producing products with as little environmental impact as possible. However, the quantification of sustainability itself is still in question leading to the question “how do we measure sustainability?” Metrics or indicators for sustainability can vary between different industries or publications and normalizing total impacts between different indicators can also lead to further variations. It is generally accepted that sustainability results from the balance between three aspects of development; economic, environmental and societal. Martins et al. [1] have developed this idea by producing four 3-D metrics that envelop all these aspects. 3-D metrics measure all three aspects of sustainability. The sustainability metrics are presented below:

- (1) Energy intensity – The energy demand of a process, typically focused on the use of non-renewable energy per unit amount of product(s)
- (2) Materials intensity – The amount of non-renewable resources required to produce the product. This includes raw materials, solvents, catalysts, etc. per unit amount of product(s)
- (3) Potential chemical risk – The amount of hazardous materials that are used in the process that can present a potential risk to human health per unit amount of product(s)
- (4) Potential environmental impact – The risk of environmental harm caused by emissions of hazardous chemicals to the environment per unit amount of product(s)

While identifying what we are looking for in terms of sustainability is an important step in developing an assessment, we still have not addressed how we will go about identifying these indicators and quantifying their ultimate impact. Even after this we need to be able to accurately compare metrics between different processes to make a final evaluation about the sustainability of a process.

The multitude of tools available allow for many different methods of performing sustainability assessments and comparative analyses of different processes. The use of process simulation packages (like Aspen Plus) allows for the accurate estimation of materials and energy requirements as well as facility emissions. The data provided by these simulations can then be normalized per unit product, making them capacity independent for comparison to similar processes.

## **2.2 Life-Cycle Assessment**

Raw materials extraction, transportation, storage, etc. are also extra steps that encompass a goods production. Life-cycle assessment (LCA) is a technique that investigates the total environmental burden a product has from cradle-to-grave. We used both Aspen Plus and LCA to produce impact data for a given product. We also formulated a multi-criteria decision matrix that can be used to compile all of the sustainability indicators into a single point value to aid in the decision making process.

Life cycle assessment is a standardized and methodological technique used to study the total environmental impact a compound has from beginning to end. With an increase in demand for environmental security and sustainability LCA has become an important tool in determining the environmental burden a product has during its entire life. This is deemed a “cradle-to-grave” methodology and covers the extraction of resources and raw

materials, the production of materials and product parts, transportation, and the use of the product as well as its final disposal. By covering the whole lifespan of a product, burdens are not allowed to be ignored or passed from one step to another. This “problem shifting” is common as environmental concerns are generally based on the fences of the production facility. Energy requirements and emissions for processes like transportation or raw material production are usually ignored in less rigorous assessments. A cradle-to-grave analysis is usually deemed a “holistic” process as it shows the interconnectedness of the whole life cycle of a chemical to the environmental burdens it entails [2].

The methods behind LCA have been internationally standardized in ISO 14040 and ISO 14044 [3, 4]. These standards layout requirements and guidelines for the definition of the goal and scope, the life cycle inventory analysis phase, life cycle impact assessment phase, interpretation phase and reporting and critical review of the LCA. The first step in an LCA is goal definition and scoping. This phase requires you to determine the product, establish the boundaries for the process and determine the environmental effects that are to be reviewed. The next phase is the life cycle inventory analysis. This is the real brunt of the work in which the energy, water and materials uses are calculated along with the environmental releases. This data is then analyzed in the impact assessment phase and are usually translated into direct potential human and ecological effects (e.g. NO<sub>x</sub> compounds emitted create acid rain which acidifies ponds causing large fish death). In the last phase the results of the inventory analysis are evaluated and a decision based on the environmental impact of the product can be made. It is also at this time that the uncertainty of the analysis is addressed. Uncertainty in an LCA comes from the assumptions made in the scope, the data (or lack thereof) and characterization factors in

the impact assessment phase [5, 6]. More detailed descriptions of the LCA process can be found in relevant literature [2, 5, 7]

A multitude of software is available for conducting life cycle assessments. Software generally contains vast databases that allow for ease of LCA application. They are also rather user friendly and help new users learn the methodology behind LCA application. Some commercial software includes GaBi, Simapro and Umberto. Freeware tools also exist such as; open-LCA, CMLCA and brightway [6]. The Argonne GREET (Greenhouse gases, Regulated Emissions, and Energy use in Transportation) model allows a user to fully evaluate well-to-wheels applications for different fuels, production strategies and vehicles. This software is also entirely free and contains a large database of raw materials extraction, fuel pathways, transportation costs and vehicles. GREET software was utilized extensively in this work.

The techniques discussed above were used to investigate the sustainability of different processes producing both chemicals and energy. The first work was in chemical looping combustion (CLC) of coal and natural gas for the efficient production of electricity with carbon capture. Sustainability metrics were investigated through Aspen Plus simulations produced. The next work is in methanol production using renewably generated hydrogen and captured CO<sub>2</sub>. A multi-criteria decision matrix was introduced in this work to show the feasibility of renewable methanol when compared to natural gas based methanol. A continuation of this methanol project was formed into the production of alternative fuels (methanol and dimethyl ether) and a life-cycle assessment on their production and use. Each of these works will be addressed in greater depth in the subsequent chapters.

It should be noted that the majority of the work in chapter 3 was taken from work published in an Energy Production Research Institute (EPRI) report [8] as well as work published in the International Journal of Energy Research [9]; the work in chapter 4 was published in Energy [10]; and a manuscript is being produced from the work in chapter 5. While there have been some additions and changes the majority of this work can be found in the referenced publications and is work originally produced by this author.

## CHAPTER 3 ENERGY SYSTEMS

### 3.1 Chemical Looping Combustion

The use of fossil fuels in the industrial era has led us to unprecedented success in terms of technology and quality of life. However, with reserves being depleted and rising levels of CO<sub>2</sub> in the atmosphere, it is important that we not only develop sources of non-fossil based energy but also find ways to reduce carbon emissions. Ambient levels of CO<sub>2</sub> have risen from 280 ppm to nearly 400 ppm since the beginning of the industrial era. While difficult to accurately predict, these levels are projected to increase to anywhere from 550 ppm to 850 ppm by the end of the century. Figure 3.1 shows that even by stabilizing emissions, CO<sub>2</sub> concentration will still rise to unsatisfactory levels [11]. Further increases in CO<sub>2</sub> concentration would cause drastic global effects including; temperature increases (2°F – 11.5°F), higher sea levels (~2 ft) and increased ocean acidity [12, 13]. The global influence presented in these effects exhibits the need for reducing CO<sub>2</sub> emissions.

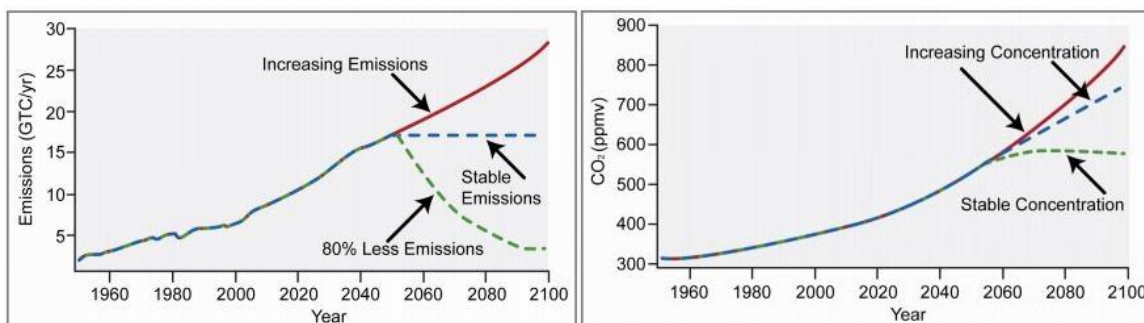


Figure 3.1: Predicted ambient atmospheric CO<sub>2</sub> concentrations compared to emissions [11]

Currently fossil fuel-based power plants account for 40% of worldwide CO<sub>2</sub> emissions.

There are three proposed methods of lowering CO<sub>2</sub> emissions and ambient CO<sub>2</sub> levels [14]:

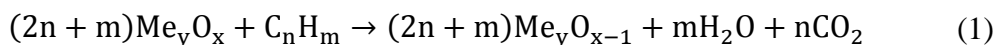
- (1) Reduce the amount of CO<sub>2</sub> produced

(2) Store or sequester CO<sub>2</sub>

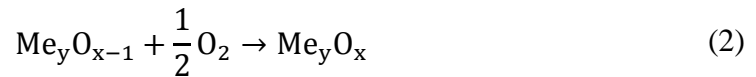
(3) Use CO<sub>2</sub> as a chemical feedstock

The first option proposed requires higher energy efficiency in energy production or the switch to more renewable based energy. The Clean Power Plan, enacted in August 2015, proposes reducing carbon emissions this way. The second option requires sequestration. This is a well-established process in which CO<sub>2</sub> is stored into deep geological formations, liquid storage sites in the ocean or via fixation into stable carbonates [15]. In the last suggested option CO<sub>2</sub> is converted into value added products. This can be a difficult process due to the inherent thermodynamic stability of CO<sub>2</sub>. Generally, high energy processes or feedstocks are required for the conversion of CO<sub>2</sub>. As these techniques can be costly, the current use of CO<sub>2</sub> industrially is mainly limited to the production of urea, salicylic acid and various carbonates [14].

Chemical looping combustion addresses the issue of carbon emissions by employing a novel method of carbon capture in energy production. By reformulating the method of oxygen delivery used in the combustion of fuels one can avoid dilution of the CO<sub>2</sub> stream with N<sub>2</sub> from the air. Chemical looping uses metal oxides (CuO, Fe<sub>2</sub>O<sub>3</sub>, NiO, CaSO<sub>4</sub>, Mn<sub>3</sub>O<sub>4</sub>, etc.) as the ultimate source of oxygen in the combustion reaction. The use of metal oxide oxygen carriers (OCs) prevents dilution of the produced CO<sub>2</sub> and H<sub>2</sub>O with N<sub>2</sub> from air. After condensation of the combustion water, a nearly pure CO<sub>2</sub> stream can be produced. A generalized form of the combustion reaction can be seen in equation 1.



where  $C_nH_m$  is some fuel and  $Me_yO_x$  is the metal oxide. The reduced metal oxide from this reaction is then oxidized back to its original state using air in a separate step. This is shown in the reaction below



The use of metal oxide in a reduction/oxidation cycle is why this system is called chemical looping. Reaction 1 is a highly exothermic reaction while reaction 2 can be either exothermic or endothermic depending on the choice of metal oxide. The hot off gas from these reactions is fed to a gas turbine for power production. An outline of this process can be seen in Figure 3.2.

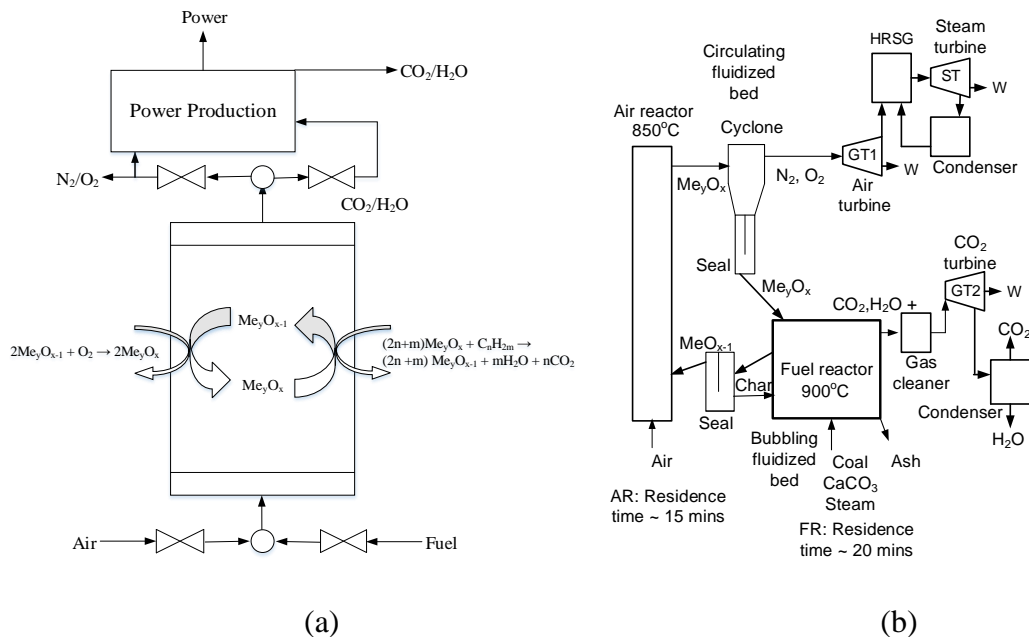


Figure 3.2: A diagram outlining the process of chemical looping combustion for power production with carbon capture in a fixed bed system (a) and a circulating fluidized bed system (b) [9]

There are two types of CLC systems; fluidized bed and fixed bed systems. These differ in how the OC is subjected to the reducing (fuel feed) and oxidizing (air feed) conditions.

Fluidized bed systems transfer the OCs between a fuel reactor and an air reactor while



fixed bed systems periodically alternate fuel and air streams in a reactor with fixed metal oxide. Regardless of reactor system there are a variety of metal oxides that can be chosen. In our work we have provided a substantial review of different oxygen carriers and fuel choices for chemical looping combustion [9]. Gaseous fuel (natural gas) is typically the easiest fuel to use because it produces very little char and no ash. Char and ash production can poison metal oxides and reduce the carbon capture efficiency. However the large supply of North American coal dictates that investigation into CLC with solid fuels is of great importance.

We chose to examine coal chemical looping combustion with two different oxygen carriers using thermogravimetric analysis (TGA), a technique often used in CLC studies [16, 17]. TGA allows the user to measure minute mass changes at varying temperatures and gas flow rates. Copper oxide and calcium sulfate were chosen as the OCs for the system. CuO has shown optimum results in many CLC studies while CaSO<sub>4</sub> has been relatively unstudied. However, the large amount of oxygen present in CaSO<sub>4</sub> is beneficial as lower amounts of metal oxide would be required to combust the coal. We ran experiments to study the conversion and reoxidation efficiencies for these metal oxides in the combustion of coal. We also produced two simulations using Aspen Plus software. These simulations use Fe<sub>2</sub>O<sub>3</sub> oxygen carriers and natural gas and coal fuel feedstocks. The simulations were produced to show the overall energy efficiency, material demands, and carbon capture that can be accomplished on a large scale CLC process. This work is presented in the subsequent sections.

### 3.2 Materials and Methods

The experimental work produced was to show the capability of using CuO and CaSO<sub>4</sub> as oxygen carriers for the combustion of coal. A thermogravimetric analyzer, TG 209 F1 Libra from Netzch, was used for all of the trials. This TGA is owned and operated by the Facility for Mechanical and Materials Characterization in Jorgensen Hall, Room 009. The system was loaded with the sample and subjected to the following heating/gas flow schedule, simulating a single oxidation and reduction cycle of chemical looping combustion, Table 3.1.

*Table 3.1: The TGA schedule ran for all of the TGA tests [8]*

Temperature (°C)	Rate (°C/min)	Gas Flow (sccm)	Time (min)
0-900	15	100 N <sub>2</sub> and 20 N <sub>2</sub>	60
900	N/A	100 N <sub>2</sub> and 20 N <sub>2</sub>	60
900	N/A	100 Air and 20 N <sub>2</sub>	60
25	-50	20 N <sub>2</sub>	30

The gas outlet port of the TGA was connected to a box holding a CO<sub>2</sub> sensor (CO<sub>2</sub>meter.com; CM-0024) and an O<sub>2</sub> sensor (CO<sub>2</sub>meter.com; CM-0202). Both sensors were attached via USB to the computer monitoring the TGA results. Before starting the TGA run the box was purged with N<sub>2</sub> gas until the sensors showed a flat response (roughly 15 minutes). The values were then calibrated to zero (at the base level) and 400 ppm at the ambient reading.

Samples consisted of a mixture of metal oxide and coal that were premixed at the specified concentrations and weighed before and after the TGA trial. Metal oxides used for these tests were CaSO<sub>4</sub> and CuO (both anhydrous). The mass ratio of CaSO<sub>4</sub> and CuO to coal used were 9.85:1 (0.94:1 mole ratio) and 22.92:1 (3.75:1 mole ratio), respectively.

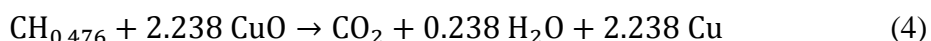
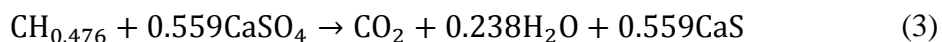
The coal used has the composition shown in Table 3.2. The ratios of coal and metal oxide were chosen as to provide excess metal oxide to the system. This should allow for complete coal combustion without interference by lack of metal oxide. The coal (Powder River Basin) used has the following composition.

Table 3.2: Proximate and ultimate analysis for the coal sample used [8]

Proximate Analysis	Weight Percent
Moisture	29.3%
Volatile Matter	28.2%
Fixed Carbon	38.8%
Ash	3.4%
<b>Ultimate Analysis</b>	
Carbon	49.6%
Hydrogen	6.7%
Nitrogen	0.7%
Sulfur	0.3%
Oxygen	37.7%
Ash	4.8%

\*Coal analysis completed by EERC on January 31, 2014

The following reactions summarize the reduction phase (first 118 minutes) of the chemical looping system.



In these reactions coal is represented as  $\text{CH}_{0.476}$  the C/H ratio of which was calculated from ultimate analysis of the coal sample. Similar empirical formulas and reactions for the combustion of coal were found in literature [16-18]. It is not made clear in many cases how empirical formulas of coal should be derived, many represent coal in a generic form as  $\text{C}_m\text{H}_{2n}$ . The oxygen present in the coal is never explicitly accounted for. Cao and Pan [16] presented a method in 2006 that assumes that the free oxygen (oxygen not in

moisture) reacts with the free hydrogen in the coal to form water. The remaining hydrogen and carbon are then used to develop a stoichiometric ratio, calculations of the CH ratio can be found in Appendix A. The following equations were used to calculate the total amount of CO<sub>2</sub> emitted.

$$V_{CO_2} = \sum_{i=1}^{745} x_{CO_2i} * Q_{carrier} * (t_{i-1} - t_i) \quad (5)$$

$$m_{CO_2} = \frac{V_{CO_2} * P}{R * T} MW_{CO_2} \quad (6)$$

where  $x_{CO_2i}$  is the concentration measured by the sensor at time interval  $(t_{i-1} - t_i)$ ,  $Q_{carrier}$  is the volumetric flowrate of the carrier gas measured by the TGA system (120 mL/min), the last term in equation 5 is the time interval that the concentration was measured in (15 seconds),  $i$  runs from 1 to 745 because there are 745 measurements per run. In equation 6,  $V_{CO_2}$  is entered in from Equation 5,  $P$  is ambient pressure (1 atm) which the gas is measured at,  $T$  is the temperature of the outlet gas measured by the sensors,  $R$  is the ideal gas constant and  $MW_{CO_2}$  is the molecular weight of CO<sub>2</sub>. Equation 6 is the ideal gas equation which should be applicable at these temperatures and pressures. Percent conversion is defined as the amount of experimental CO<sub>2</sub> released divided by the theoretical CO<sub>2</sub> produced

$$\% \text{ Conversion} = \frac{\text{Experimental CO}_2}{\text{Theoretical CO}_2} * 100 \quad (7)$$

Theoretical CO<sub>2</sub> was calculated by using the coal analysis given in Table 3.2. The total amount of carbon present in the coal was calculated by multiplying the dry weight of the coal by the percent of carbon in the coal. Assuming all of the carbon is converted into

carbon dioxide we are able to assume a 1:1 molar ratio between moles of carbon in the coal and moles of CO<sub>2</sub> theoretically emitted. This equation can be seen below.

$$\text{Theoretical CO}_2 = \text{mass}_{\text{coal}} * (1 - x_{\text{moisture}}) * x_C * \frac{MW_{\text{CO}_2}}{MW_C} \quad (8)$$

Table 3.3 summarizes the results of the reduction part of these tests.

*Table 3.3: Results of the reduction phase of the chemical looping trials [8]*

	Coal used* (mg)	Theoretical CO <sub>2</sub> (mg)	Experimental CO <sub>2</sub> (mg)	% Conversion
CuO	4.187	5.379	5.114	95.1%
CaSO <sub>4</sub>	8.245	10.591	10.246	96.7%

\* The mass ratio of CaSO<sub>4</sub> and CuO to coal used were 9.85:1 (0.94:1 mole ratio) and 22.92:1 (3.75:1 mole ratio), respectively

During the reoxidation stage (past 118 minutes) the reduced metal oxide reacts with oxygen to reform our original metal oxide, see reactions below.



By calculating the amount of metal oxide present after the reformation stage and comparing to the original amount of metal oxide we can calculate the % reoxidation, see equation 11.

$$\% \text{ Reoxidation} = \frac{\text{MeO after Reforming}}{\text{Initial MeO}} * 100 \quad (11)$$

The calculation of remaining metal oxide will be discussed in the discussion section as we have postulated that reactions 3, 4, 9 and 10 are not the only reactions occurring. A summary of the reformation results can be found in Table 3.4.

Table 3.4: Results for the reoxidation section of the chemical looping trials [8]

	Initial MeO (mg)	MeO after reformation (mg)	% Reoxidation
CuO	95.974	78.165	81.4%
CaSO <sub>4</sub>	81.221	65.331	80.4%

### 3.3 Discussion

#### 3.3.1 CuO Trials

The CuO trials appeared to behave very similar to results found in literature. Results of mass loss and CO<sub>2</sub> emission can be seen in Figure 3.3. It should be noted that at 118 minutes air is introduced. The mass gain at this time period is due to the oxidation of the reduced metal oxide.

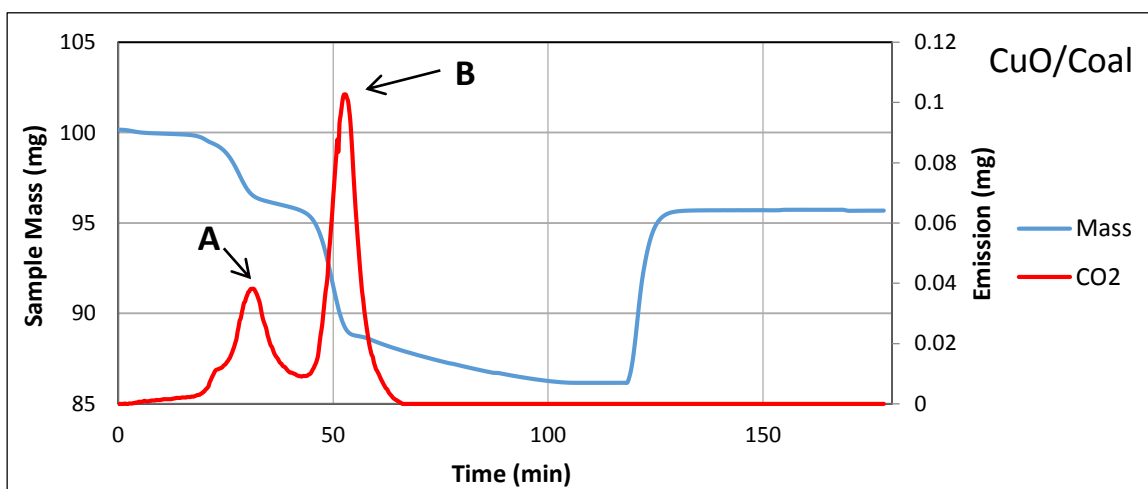


Figure 3.3: Experimental data showing the mass loss and CO<sub>2</sub> emissions for a CuO/coal sample [8]

There is an initial phase (peak A in Figure 3.3) in which volatile matter is combusted and a second peak that is the result of further combustion of the solid matter of the coal (peak B in Figure 3.3). Also observed is a gradual decrease in mass while no CO<sub>2</sub> is being

emitted (from roughly 70 minutes to 100 minutes). This phenomenon has been observed in similar TGA experiments [16, 19] and is assumed to follow the reaction below.



This reaction is said to occur at temperatures slightly below 900 °C. As the system is in this temperature range and constantly removing the expelled oxygen by purging the system with the N<sub>2</sub> flow; it is possible that this reaction does occur. The extent of this reaction was calculated using an Excel spreadsheet. After calculating the mass loss that would occur with the CO<sub>2</sub> released (measured by our sensor) we then calculated the remaining CuO that could react according to equation 12. An initial guess was made for the conversion of the reaction and the mass remaining in the sample (unreacted coal, ash, formed Cu, formed Cu<sub>2</sub>O and unreacted CuO) was calculated. The solver function in Excel was then used to minimize the error between the calculated and experimental variables (i.e. residual mass, mass loss, and CO<sub>2</sub> emission) by changing the % combustion and % conversion.

The amount of reformed CuO was then calculated by assuming all of the mass gain during the oxidation section was the result of O<sub>2</sub> reacting with the sample. The study of the mechanism and kinetics of the oxidation of Cu at high temperatures has been widely studied. At 900 °C and ambient partial pressures of O<sub>2</sub> the mechanism proceeds by forming Cu<sub>2</sub>O scale and then further oxidation of this Cu<sub>2</sub>O to CuO [20] Based on this mechanism we have assumed that the Cu first reacts to Cu<sub>2</sub>O and then subsequently the CuO is formed from this Cu<sub>2</sub>O. The calculations for reduction and oxidation sections can be found in Appendix A.

### 3.3.2 CaSO<sub>4</sub> Trials

Similar data was gathered for the CaSO<sub>4</sub> and coal trial. These results can be found in Figure 3.4.

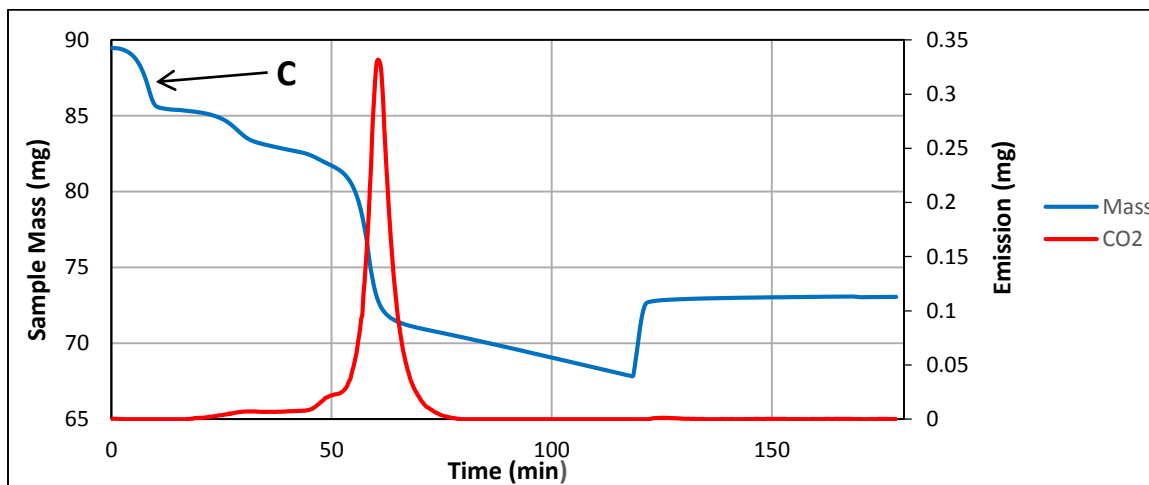


Figure 3.4: Experimental data showing the mass loss and CO<sub>2</sub> emissions for a CaSO<sub>4</sub>/coal sample [8]

It is clear that the CaSO<sub>4</sub> trial shows different results especially in the mass loss curves and the CO<sub>2</sub> production peaks. There are three mass loss events in the reduction phase of the CaSO<sub>4</sub> trials. The first (point C in Figure 3.4) we have attributed to water evaporation from the sample. The first event happens at an oven temperature between 100 and 200 °C which is in the range for water evaporation. It can also be seen that the CO<sub>2</sub> levels do not change during this mass loss and is likely not due to combustion or volatilization. We believe that the majority of the water lost is not from the coal but from the CaSO<sub>4</sub>. As received the CaSO<sub>4</sub> is anhydrous but it readily picks up water from the air. This is evident during weighing as the sample gains mass for a long time before stabilizing to a final value. We ran a blank trial with a sample only containing CaSO<sub>4</sub> and a similar mass loss was observed (see Figure 3.5).



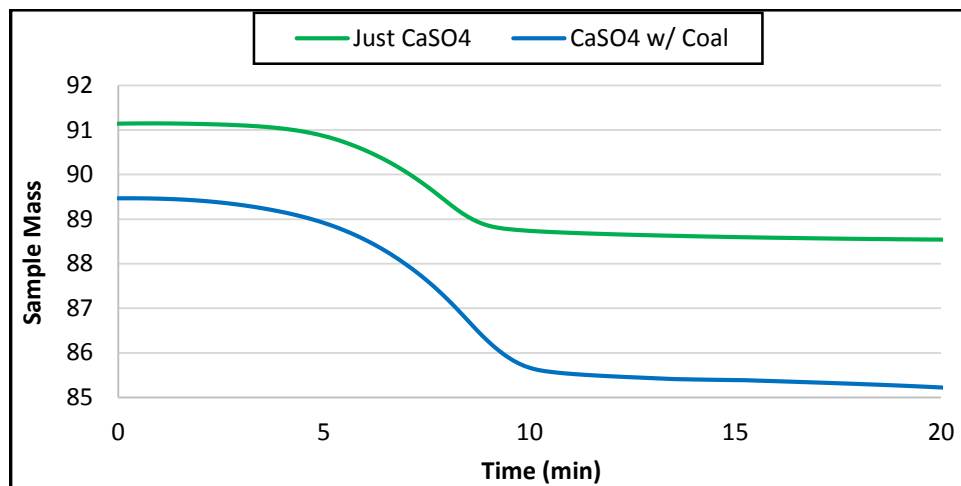
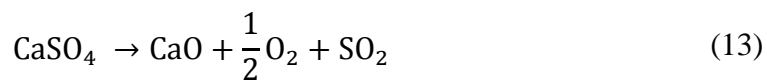


Figure 3.5: A comparison between the  $\text{CaSO}_4$  blank (green) and a  $\text{CaSO}_4$  and coal sample (blue) showing mass loss attributed to water evaporation [8]

The water loss for the blank sample was calculated (assuming all water evaporation occurs between 0 and 10 minutes). The water loss was applied to our  $\text{CaSO}_4$  and coal trial calculations by standardizing the loss to the mass of  $\text{CaSO}_4$  in the sample.

However, calculations show that the remaining mass loss is not solely from combustion products, and thus we have concluded that thermal degradation must be occurring. Much like in the  $\text{CuO}$  trials a mass loss event occurs without  $\text{CO}_2$  emission (between 70 and 118 minutes) in the  $\text{CaSO}_4$  trial. The release of  $\text{SO}_2$  is one of the major concerns for using  $\text{CaSO}_4$  based oxygen carriers in chemical looping systems. The most common reaction is shown below.



It has been shown that this reaction only significantly occurs at temperatures greater than  $1200^\circ\text{C}$ , even when no  $\text{SO}_2$  is present in the atmosphere [65]. As well there was no observed increase in  $\text{O}_2$  levels in the off gas. It is for these reasons that we do not believe

this reaction is occurring. Another likely reaction is the solid-solid reaction that occurs between  $\text{CaSO}_4$  and  $\text{CaS}$ .



The  $\text{CaS}$  formed from reaction 3 and the excess  $\text{CaSO}_4$  in the sample could be going through this reaction. This reaction also occurs at a maximum rate between 800 and 900 °C and has been thermodynamically and experimentally examined in previous work [21]. In our experiment we believe that this reaction is occurring and limiting the reoxidation of the  $\text{CaSO}_4$ . The near linear slope between 60 and 120 minutes leads us to believe that this reaction does not proceed to completion. A similar method of determining the % combustion and conversion for the  $\text{CuO}$  was done for the  $\text{CaSO}_4$  trial. Again, mass loss due to the reactions (3 and 14) and residual mass were calculated for guesses of % combustion and conversion. Similarly the errors were minimized using Excel's solver function to attain the final values. Calculations can be found in the Appendix A.

### 3.4 CLC Simulations

Two simulations of chemical looping combustion process were modeled using Aspen Plus [22] and the its carbon tracking tool; one using light natural gas (LNG) as an input and the other using coal. Both plants use iron as the oxygen carrier and a three-reactor system consisting of a fuel reactor, oxidizer, and air reactor (see Figure 3.6 and Figure 3.7). The OC is cycled through these reactors and reacts with coal, water, and air, respectively. Each of the reactors is modeled using an RGibbs reactor that minimizes the Gibb's free energy of the system at the specified temperature and pressure to estimate the equilibrium compositions. Pressures, temperatures, and flow rates were optimized to ensure complete oxidation/reduction of the oxygen carriers, while maximizing energy

production. The next sections summarize the individual simulations, with a comparison between the two on a per energy basis discussed.

### 3.4.1 Coal CLC plant

The coal fired CLC plant can be seen in Figure 3.6. The plant uses 12.5 mt/hr of coal with proximate and ultimate analysis seen in Table 3.2.

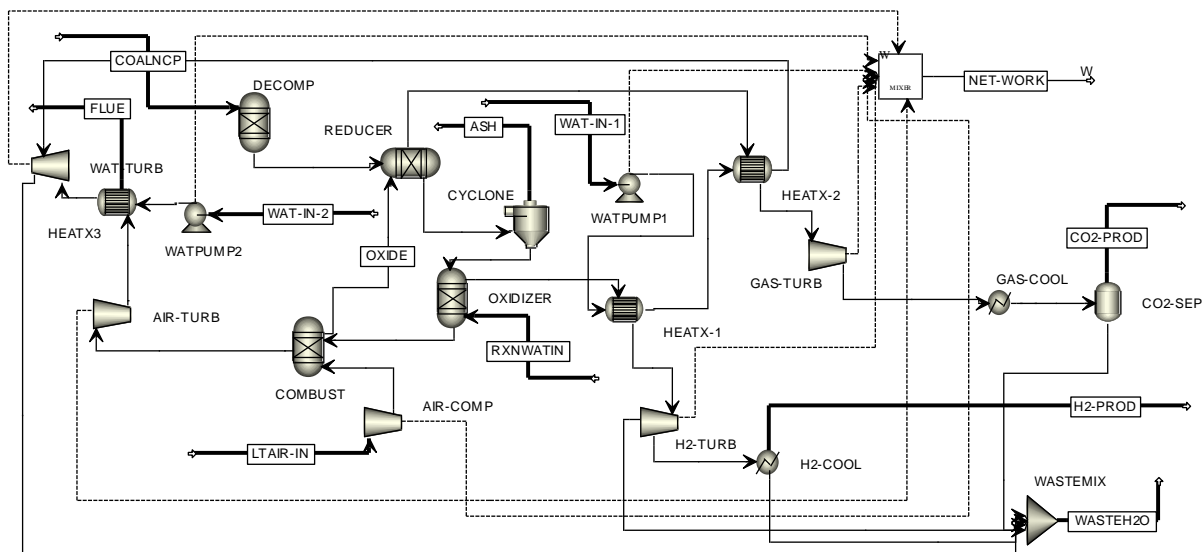


Figure 3.6: Process flow diagram of the coal based CLC plant; streams in bold represent inputs and outputs [9]

The coal and ash are defined as nonconventional solid components. We first decomposed the coal, using a RYield reactor, into its constituent elements based on the ultimate analysis. This stream reacts with a 126 mt/hr  $\text{Fe}_2\text{O}_3$  stream called OXIDE in the REDUCER reactor, where the coal is combusted and the  $\text{Fe}_2\text{O}_3$  is reduced to primarily FeO with some  $\text{Fe}_3\text{O}_4$ . This reactor is operated at 900 °C and 22 atm. The gas stream travels through a heat exchanger, turbine, and a cooler before separating into a semi-pure  $\text{CO}_2$  stream. The ash and solids are separated using a cyclone, and the metal oxide travels to the OXIDIZER reactor where 20 mt/hr water is added to oxidize the FeO to  $\text{Fe}_3\text{O}_4$  and

produce  $H_2$  gas. This is a lot of water, but it is required to produce the hydrogen gas. However, if  $H_2$  production is not desired, this reactor can be bypassed and the oxygen carrier can be reformed in the COMBUST reactor. As well, conditions of this reactor can be varied to produce more energy or more  $H_2$ . For this simulation we chose to operate at 30 atm with a duty of 0 MW. The vapor stream, consisting of  $H_2$  and water, travels through a heat exchanger, turbine, and cooler to produce a relatively pure  $H_2$  stream. The solids travel onto the COMBUST reactor where 21.6 mt/hr of compressed air is added to the hot  $Fe_3O_4$ . The reactor operates at the same conditions as the OXIDIZER reactor. The oxygen from the air reacts with the  $Fe_3O_4$  and produces the  $Fe_2O_3$  that loops back to the beginning of the process and reacts with the coal input. The gas stream, high temperature oxygen depleted air, travels through a heat exchanger and is released into the atmosphere. Throughout this process most of the heat is captured via heat exchanger and transferred to water streams to produce steam. These steam streams are then fed to a turbine to produce electricity. Other sources of electricity are from the turbines that depressurize the  $CO_2$  and  $H_2$  streams. The produced and consumed electricity of the process are combined and have been visualized in the process as the NET-WORK stream, which produces 5.42 MW of electricity. This value can be varied depending on the operating conditions chosen for the reactors and the desired amount of  $H_2$  produced. Along with electricity, this plant produces 1 mt/hr of a 99.9%  $H_2$  stream at 30 bar. As well the plant suppresses the  $CO_2$  produced into a 15.9 mt/hr stream that is 83.9 mol%  $CO_2$ . This  $CO_2$  stream could be further purified and sold, or sequestered by normal procedures. Input and output streams, utilities usage, and overall mass and energy balance for this simulation can be found in Appendix A.

### 3.4.2 LNG CLC plant

The light natural gas plant operates in a similar fashion as the coal plant but acts as a cogeneration plant, producing heat as well as electricity (Figure 3.7). Nonetheless, the chemical looping aspect of this plant is the same. The plant starts with a 15.2 mt/hr natural gas stream at  $-162\text{ }^{\circ}\text{C}$  and 2 bar composed of 95 mol% methane, 2 mol% ethane, 1 mol% propane and 2 mol%  $\text{N}_2$ . This stream feeds directly into the REDUCER where it reacts with a 670 mt/hr  $\text{Fe}_2\text{O}_3$  stream. This reactor operates at 14 bar and  $1000\text{ }^{\circ}\text{C}$ . The gas stream goes through a turbine and heat exchanger before condensing into a 98 mol%  $\text{CO}_2$  product stream. The metal oxide then travels to the OXIDIZER where it reacts with a 63 mt/hr steam stream at 22 bar and  $375\text{ }^{\circ}\text{C}$  that is produced later in the process. This reactor operates at 22 bar and  $300\text{ }^{\circ}\text{C}$  and the excess heat from this reactor goes to heat collection. The gas stream, primarily  $\text{H}_2$  and water, runs through a turbine before being condensed and compressed into a 99.96 mol%  $\text{H}_2$  product stream. The metal oxide, now entirely  $\text{Fe}_3\text{O}_4$ , is sent to the COMBUST reactor where it reacts with a 245 mt/hr compressed air stream. This reactor operates at 22 bar and  $950\text{ }^{\circ}\text{C}$ . The depleted air is sent to a turbine and heat recovery system before being emitted into the atmosphere and the metal oxide, now  $\text{Fe}_2\text{O}_3$ , is sent back to react with more LNG.

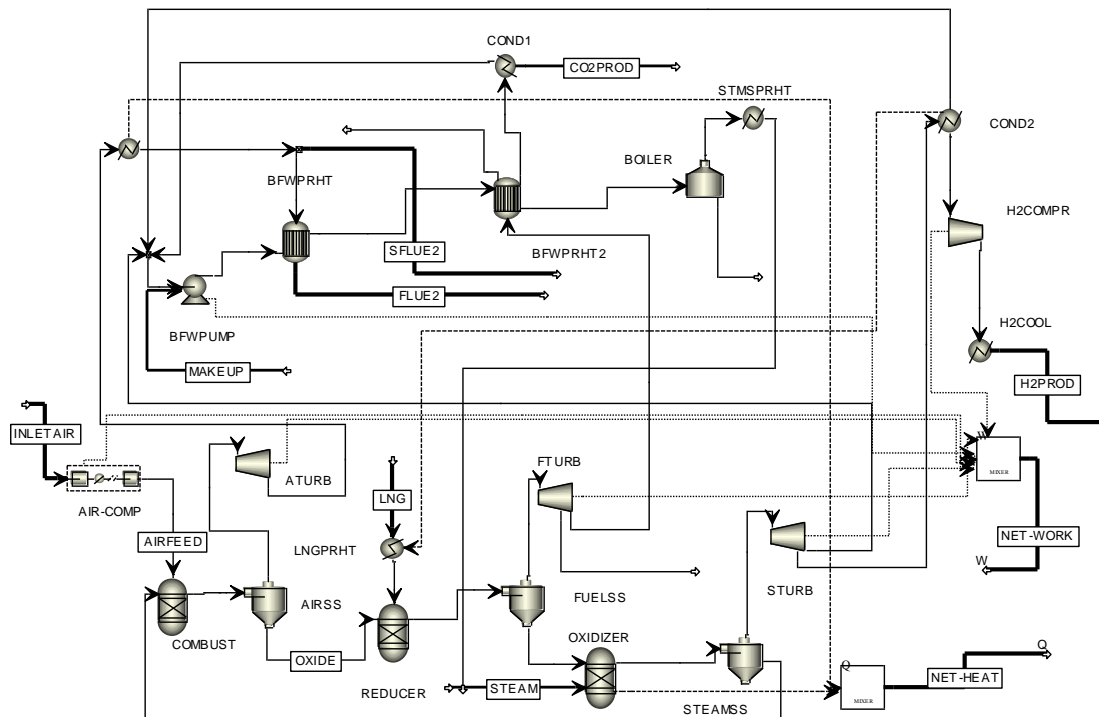


Figure 3.7: A LNG based CLC cogeneration plant where again bolded streams are inputs and outputs [9]

Much like the coal plant, this plant produces electricity by using turbines to depressurize streams. All of the electricity produced and generated is added together in the NET-WORK stream. Altogether, the plant produces a total of 17.8 MW of electricity.

However, this plant also produces 159.4 MW of heat that can be used to produce hot water or more steam for energy production. As well, the plant also produces a 5.3 mt/hr stream of 99.96 mol% hydrogen gas at 30 bar and 45.4 mt/hr of a 98 mol% CO<sub>2</sub> stream.

Input and output streams, utilities usage, and an overall mass and energy balance for this simulation can be found in Appendix A.

### 3.5 Sustainability Metrics of the CLC plants

While both of these simulations could undergo further optimization to produce more energy and improve efficiency, it is clear that both plants greatly overshadow common

energy production plants in terms of environmental impacts. The LNG and coal plants have low CO<sub>2</sub> emissions at 3.14 and 3.65 mts of CO<sub>2</sub> equivalents per MWhr of energy produced, respectively. It is also important to note that the CO<sub>2</sub> produced in these plants is stored in a nearly pure CO<sub>2</sub> product stream and not emitted into the atmosphere. This being said, if this CO<sub>2</sub> were to be sequestered or converted into another compound the CO<sub>2</sub> emissions of the plants could be reduced even further. Essentially only the only CO<sub>2</sub> emissions would be from the utilities resulting in emissions of 1.73 and 0.90 mts of CO<sub>2</sub>/hr for the LNG and coal plants respectively. Comparatively, between the two CLC plants, a safe assumption would be that the LNG plant is more environmentally sustainable. However, while the LNG plant produces more electricity/heat and has a lower CO<sub>2</sub> emissions, it should be noted that the plants operate on different scales and are innately different. The LNG plant uses an equivalent of 12240 mt/hr of carbon where the coal plant uses 6206 mt/hr; nearly half the amount. As well, the coal plant uses heat to produce steam for electricity whereas the LNG plant produces raw heat. The plants differ greatly on utility usage, with the coal plant requiring less than 10% of the required heating and cooling duty of the LNG plant. However, by normalizing on a per energy basis, the plants are very comparable. This data can be seen in Table 3.5. Each of the plants produces product streams of hydrogen and CO<sub>2</sub>. Utilities and carbon tracking was done using the US-EPA-Rule-E9-5711 to determine CO<sub>2</sub> equivalents (CO<sub>2</sub>e).

Table 3.5: Sustainability metrics for the CLC simulations using coal and natural gas [8]

Sustainability metrics	LNG CLC Plant	Coal CLC Plant
<b>Material metrics</b>		
Material input (mt of C/hr)	12240	6206
Net H <sub>2</sub> production (kmol/hr)	2640	492
Net H <sub>2</sub> production/Unit electricity produced (kmol/MWhr)	82.97	90.8
Net CO <sub>2</sub> captured (kmol/hr)	1020	338.7
Net CO <sub>2</sub> captured /Unit electricity produced (kmol/ MWhr)	32.06	62.5
<b>Energy intensity metrics</b>		
Net electricity production (MW)	31.8	5.42
Net heat production (MW)	159.4	N/A
Total heating duty (MW)	232.8	20.67
Total cooling duty (MW)	233.4	12.07
Net duty (heating- cooling) (MW)	-0.6	8.60
Total heating cost (\$/hr)	3931.64	238.02
Total cooling cost (\$/hr)	3621.82	187.37
Net cost (heating + cooling) (\$/hr)	7553.46	425.39
<b>Net cost/Unit electricity produced (\$/MWhr)</b>	<b>237.40</b>	<b>78.49</b>
<b>Environmental impact metrics</b>		
Net stream CO <sub>2</sub> (mt/hr)	44.89	14.91
Utility CO <sub>2</sub> (mt/hr)	55.12	4.90
Total CO <sub>2</sub> (mt/hr)	100.01	19.80
Total CO <sub>2</sub> /Unit electricity produced (mt/MWhr)	3.14	3.65
Total CO <sub>2</sub> /Net heat produced (mt/MWhr)	0.63	N/A
Total CO <sub>2</sub> /Net H <sub>2</sub> produced (kg/kmol)	37.88	40.25
Net carbon fee (\$/hr)*	200.01	39.60
Net carbon fee/Unit electricity produced (\$/MWhr)	6.29	7.31

\* The carbon fee was assumed to be \$2/mt of CO<sub>2</sub>e.

### 3.6 Conclusions

Chemical looping technology offers a unique approach to the difficult problem of efficient carbon capture in energy production. By avoiding N<sub>2</sub> flue gas dilution chemical looping combustion is able to produce energy while capturing and producing a relatively pure CO<sub>2</sub> stream. Both gaseous and solid fuels can be used in these systems. Through Aspen Plus simulation it was shown that CO<sub>2</sub> emissions can be greatly reduced using CLC methods. Normalized to a per MWhr electricity produced basis, coal and natural gas fuels only emit 3.65 and 3.14 mt of CO<sub>2</sub>e, respectively. Coal and natural gas based CLC produces electricity with utilities costs of 7.8¢/kWhr and 23.7 ¢/kWhr, respectively. Two potential oxygen carriers, CuO and CaSO<sub>4</sub>, were experimentally subjected to a chemical



looping routine using thermogravimetric analysis. Coal was chosen as the fuel of choice. High fuel conversions (95-96%) were found for both MeOs. However reoxidation is a concern at the conditions used in these trials. Potential side reactions limit the reoxidation of both MeOs. Due to the cycling of metal oxide required in these systems low reoxidation of MeOs makes this process highly infeasible. As well effective methods for cycling metal oxides between fuel and air reactors is required before an industrial scale facility is realized. Future work is suggested to optimize the time and temperature of combustion and reoxidation for both oxygen carriers. The mixed ratio of coal to MeO should also be investigated and there exists a need for a more detailed description of the coal/MeO surface phenomena and reaction. Nonetheless the work presented in this chapter shows the exciting potential that CLC may have on the energy sector. The sustainability of these systems warrants an increased investigation into their feasibility.

## CHAPTER 4 CHEMICAL PROCESS INDUSTRIES – METHANOL PRODUCTION

### 4.1 Introduction

The generation of renewable electricity suffers from intermittent and fluctuating character and necessitates the storage. Wind energy-based electrolytic hydrogen may serve as a chemical storage for renewable electricity[23-27]. Hydrogen is a clean fuel, its burning causes no harmful emissions, and it has a gravimetric heating value three times higher than typical hydrocarbon fuels [23, 24]. On the other hand, the cost to produce, store, compress, and transport hydrogen is still high[28-31]. CO<sub>2</sub> conversion with H<sub>2</sub> can not only store the wind power used in hydrogen production but also fix carbon dioxide.

The result of CO<sub>2</sub> hydrogenation reactions is highly dependent on the catalyst, operating conditions and reaction time. The products of these reactions can include; hydrocarbon fuels, formic acid, methyl formate, formamides, carboxylic acids, and methanol [32-36]. Due to its low production costs, well established infrastructure and advanced processing technology, methanol is an ideal candidate for the conversion of CO<sub>2</sub> and H<sub>2</sub> [27].

Methanol, also called methyl alcohol or wood alcohol, is the simplest aliphatic alcohol having the chemical structure CH<sub>3</sub>OH. It is a volatile, clear liquid at room temperature and is miscible with water. However, it is flammable and toxic. Methanol is a global commodity. With over 90 plants worldwide the current production capacity is near 100 million metric tons (MMT). Each day roughly 100,000 tons of methanol is used [37].

Methanol is used as a chemical feedstock in the production of many chemicals including; formaldehyde, acetic acid, methyl amines and methyl chloride. When used in this fashion the CO<sub>2</sub> utilized in methanol synthesis is fixed into these chemicals. Methanol also plays

a valuable role in the energy sector and can be used as a direct fuel or fuel additive. In this case the CO<sub>2</sub> fixed into methanol would be recycled.

The earliest use of methanol can be traced back to ancient Egypt in which it was unknowingly created as a byproduct of wood pyrolysis. Along with other chemicals it was used as a part of the embalming process. It would be centuries later in 1664 when its pure form was first isolated and even later in 1834 for it to be chemically identified.

Arguably the largest stride in the history of methanol would be when chemist Matthias Pier was able to reform methanol from synthesis gas (syngas) in 1923 [38].

Since this discovery the production of methanol has skyrocketed, mostly using improved versions of this process. Current global methanol demand is around 70 million metric tons with a projected demand of 137 MMT by 2022 [39, 40]. Recently the demand for methanol has shown a substantial increasing trend. The emergence of Lurgi

MegaMethanol® plants and other large scale methanol production facilities has been able to meet this demand. These large scale plants usually use natural gas as the source of syngas. There is naturally an economic correlation between natural gas prices and oil prices and consequently oil prices and methanol prices (see Figure 4.1). As fossil fuel sources are depleted, prices of natural gas (and other fossil fuels) will continue to increase ultimately leading to an increased methanol production cost [41, 13].

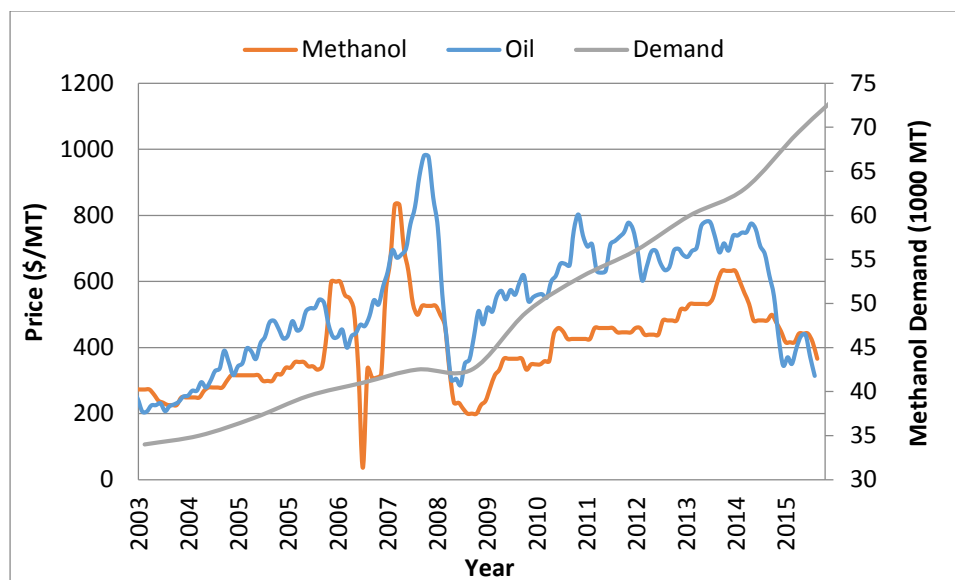


Figure 4.1: Methanol price and demand in recent history[40 ,42, 43].

The use of renewables in the production of methanol would not only alleviate the issues associated with an increase in fossil fuel cost but would eliminate methanol’s dependency on fossil fuel feedstocks. Since methanol can be used as a fuel source itself, its production from renewables would help to recycle CO<sub>2</sub> and reduce the reliance of our energy and transportation sectors on fossil fuels. Olah [39] presents this idea in a very concise term called the “Methanol Economy”. Put short, this concept purveys the idea that methanol can be used as an alternative way for storing, transporting and using energy [44, 45].

Methanol is also a valuable chemical feedstock commodity. The main use for methanol (roughly 30% of world demand) is for its conversion into formaldehyde. Other notable chemical commodities would be acetic acid, dimethyl ether (DME), methyl-tert-butyl ether (MTBE), and olefins (ethylene and propylene) [46]. A more complete list of the demand for methanol can be seen in Figure 4.2. After an initial conversion to value added chemicals and then further conversion into final products, methanol deployment stretches

into thousands of products including; plastics, Plexiglas, resins, solvents, adhesives, insulation, particle board, paints and more.

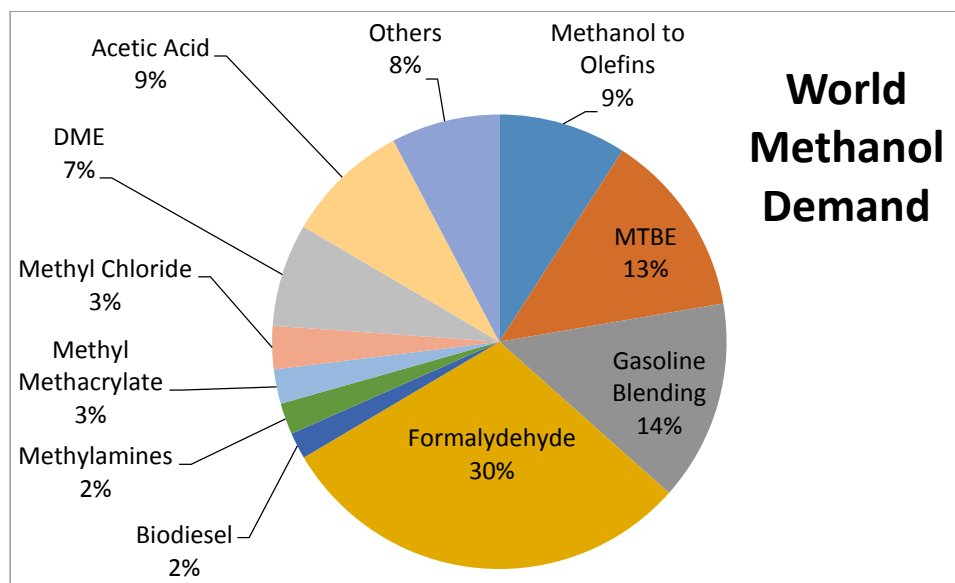


Figure 4.2: World methanol demand according to use [46].

Rihko-Struckmann et al. [47] carried out an energetic evaluation in order to assess the overall efficiency of methanol and hydrogen-based storage systems for renewable electric energy; the efficiency of the system using hydrogen is higher compared with that of using methanol as storage medium; however, storage and handling of methanol as chemical storage is favorable when compared with H<sub>2</sub>. Tremel et al. [27] investigated the economics of producing five fuels from electrolytic hydrogen. Of these five fuels, methanol performed the best overall, receiving high marks in terms of economics and technology. CO<sub>2</sub> hydrogenation has also been simulated by Van-Dal and Bouallu [48, 49] showing that the production of methanol can fix large quantities of CO<sub>2</sub>. The production of hydrogen using carbon free electricity was highly stressed in these papers, as if as little as 20% of the electrolysis energy is the result of a coal fired plant the CO<sub>2</sub> abatement

becomes null. As well Pontzen et al. [50] studied methanol production from CO<sub>2</sub> and H<sub>2</sub>, showing that CO<sub>2</sub> fixation can be achieved using a commercial Cu/ZnO/Al<sub>2</sub>O<sub>3</sub> catalyst and is possible on a large scale. However, a main concern listed is the associated costs and energy of producing and purifying CO<sub>2</sub> and H<sub>2</sub> again using carbon neutral sources. Mignard et al. [51] conducted an economic feasibility study of a methanol production using CO<sub>2</sub> and renewable electricity in 2003. However they used CO<sub>2</sub> from flue gas and did not specify the source of the renewable electricity, only set a flat price of 0.015 £/kWh (2003 £).

This study is for the feasibility analyses of methanol production using wind-based electrolytic hydrogen and CO<sub>2</sub> captured from an ethanol plant. Electricity from wind power is used since its levelized cost is comparable with hydropower, and around 38% lower than that of solar photovoltaic as seen in Appendix B [24, 23]. Costs and energy requirements are calculated for wind-based H<sub>2</sub> and ethanol-based CO<sub>2</sub> production, compression, and storage. The economic feasibility of methanol plant using these inputs is investigated with varying production costs of electrolytic hydrogen and methanol selling prices. We believe sustainability to be a topic of great importance that should be included in feasibility analyses. A multi-criteria decision matrix has been created to include sustainability metrics, along with economic factors, in feasibility analyses. The renewable methanol option is compared with conventional fossil fuel-based methanol synthesis using this multi-criteria decision matrix.

## 4.2 Conventional Methanol Production

### 4.2.1 Syngas Production

Currently commercial methanol production is based on fossil fuel feedstocks. There are a variety of processes for how this is done but the general procedure follows these four steps; syngas production, syngas cleanup, methanol formation, purification. Syngas is a mixture of primarily carbon monoxide and hydrogen gas with some carbon dioxide as well. Depending on the choice of feedstock and operating conditions, different reactions may occur. The most common procedure for coal is gasification. Equations 15 and 16 present the partial oxidation and steam reforming of the carbon present in the coal.



Natural gas (primarily methane) has three common routes for producing syngas. Equation 17 presents the most common method in steam reforming. Equation 18 shows the partial oxidation of methane and Equation 19 is dry reforming. There are various reasons for choosing different reforming techniques including plant size, the ratio of CO to H<sub>2</sub> desired, and capital investment.



All of these reactions produce some variation of syngas. Depending on the content of original feedstock, the syngas usually requires additional processing. For optimal methanol synthesis the ratio of CO to H<sub>2</sub> in the syngas should be roughly 1:2. This ratio

can be adjusted by the addition of more H<sub>2</sub> or through the water gas shift (WGS) shown in reaction 20.



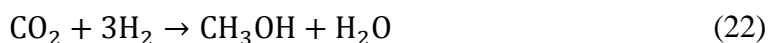
Due to impurities (sulfur, ammonia, chlorides, mercury, etc.) in the coal or natural gas feedstock, additional steps are required to clean the syngas before it is reformed into methanol. The contaminants need to be removed to pass environmental regulations as well as to protect downstream processes, especially methanol catalysts. Woolcock et al. [52] provide a substantial review in the area of syngas cleanup. Cold gas cleanup is the most mature technology primary utilizing wet scrubbers to remove contaminants. However many additional unit operations are used including cyclones, chemical solvent absorbers, and activated carbon scrubbers. A major issue with syngas cleanup is these technologies develop large waste streams and can suffer from low efficiencies.

#### **4.2.2 Methanol Conversion**

After cleanup, the syngas is passed to a reactor in which methanol is formed. Most industrial methanol production processes utilize a Cu-based catalyst, usually mixed with ZnO on an Al<sub>2</sub>O<sub>3</sub> support. However there are numerous studies on how other catalyst formations including; Cu/ZnO/ZrO<sub>2</sub>, Cu/ZrO<sub>2</sub>, Cu/Cr<sub>2</sub>O<sub>3</sub>/Al<sub>2</sub>O<sub>3</sub> and Ag/ZrO<sub>2</sub> as well as the addition of promoters (e.g. TiO<sub>2</sub>, SiO<sub>2</sub>, Na<sub>2</sub>CO<sub>3</sub>) can influence methanol production [53]. The industrial Cu/ZnO/Al<sub>2</sub>O<sub>3</sub> catalysts offer high activities and high selectivities (~99%), which is important because of the amount of unwanted byproducts (methane, ethane, higher order alcohols, etc.) that can be formed.



The mechanism for methanol production is still rather disputed but we do know that reactions 21 and 22 are the main reactions involved in methanol production. As would be expected the WGS (reaction 20) is also involved.



Both reactions 21 and 22 are exothermic producing 90.8 and 49.6 kJ/mol, respectively. There are a large variety of reactor technologies that exist. All of these technologies are very similar but deal with the heat of reaction differently. They can be classified into three main categories; quench reactors (Mitsubishi Gas Company), adiabatic reactors in series (ICI), and boiling water reactors (Lurgi) [54]. Effective use of this process heat can lead to high energy/exergy efficiencies in this process. Single pass conversions usually approach 50% [55].

#### **4.2.3 Methanol Purification**

Separation technologies consist of a series of flash drums and distillation columns. A flash drum after the reactor removes most of the unreacted gases. These are recompressed and sent back to the reactor. The liquid passes on to the first distillation column in which separates the light ends in the distillate. The bottoms is fed to a second distillation column in which the product methanol is separated out [56]. An example flow diagram of this methanol production process can be found in Figure 4.3.

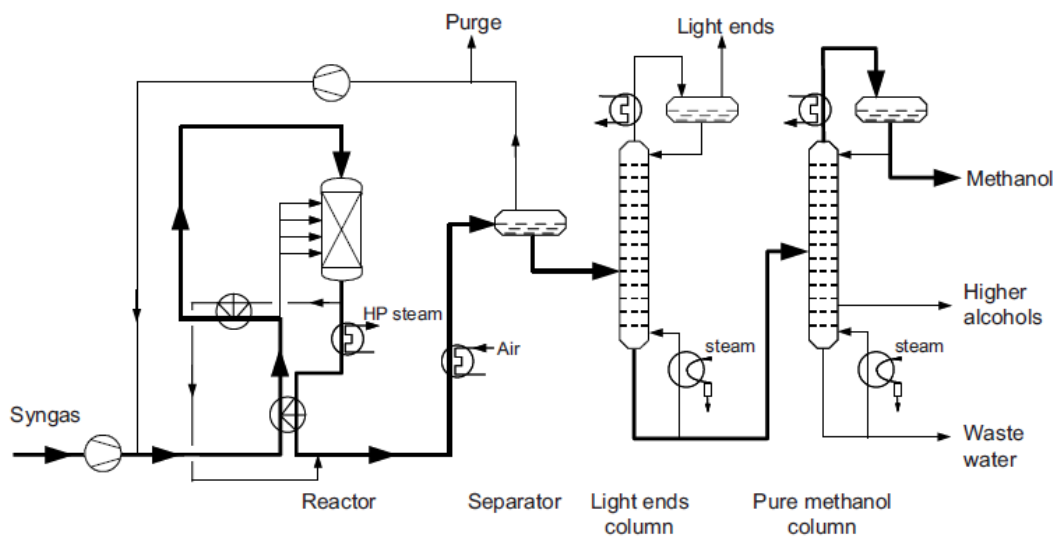


Figure 4.3: A flow diagram presenting the ICI low pressure methanol synthesis [56]

While the industrial production of methanol in this fashion represents the most advanced technology we have available, it is still suffering from the fact that it relies of fossil fuel feedstock.

### 4.3 Green Production

There are many routes of methanol production utilizing renewable inputs. An overwhelming number of papers have been recently published focusing on the thermochemical conversion of biomass feedstocks. This technology is very similar to conventional methanol production however the gasification of biomass is used to produce syngas [57, 58]. This syngas can then be subjected to a similar process as conventional methanol. However gasification technologies are far from the only strategy for renewable methanol production.

Shamsul et al. [59] provide a substantial review on the production of biomethanol from renewable sources. Biomass feedstocks vary from agricultural waste, forestry waste, livestock and poultry waste, fishery waste and sewage sludge. A vast collection of

conversion strategies are highlighted including; pyrolysis, gasification, biosynthesis, methane, CO<sub>2</sub>/CO and photo-electrochemical (PEC) processes. While all of these approaches have their own benefits they also have shortcomings. The direct use of biomass (in pyrolysis and gasification) causes problems due to feedstock variability, moisture content and syngas cleanup. Biosynthesis, direct methane conversion and PEC processes are all still in their infancy and no commercial technology could be found by this author. However the conversion of CO<sub>2</sub> with hydrogen presents an interesting concept that avoids the downfalls of the technologies addressed above.

#### **4.3.1 H<sub>2</sub> Production**

We have chosen to investigate wind-based electrolytic hydrogen and CO<sub>2</sub> produced from an ethanol fermentation process. Electrolysis is one of the oldest processes used for the production of pure H<sub>2</sub> gas. The process is typically two coupled redox reactions devolved from the splitting of a water molecule. The net reaction can be seen in equation 23.



This process requires a lot of energy (typically in the form of electricity). In order to be considered a renewable process this electricity must come from renewable sources such as; hydropower, wind power, or solar photovoltaic power. We have chosen to investigate wind energy over the rest of these renewable energy processes. Wind based electricity has one of the lowest total levelized costs of renewably based electricity [10]. It was also chosen because wind based electrolysis shows the lowest environmental impacts of these technologies [60, 61].

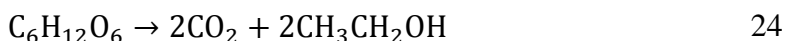
Alkaline electrolysis technologies are the most mature commercial systems. The system includes the transformer, thyristor, electrolyzer unit, feed water demineralizer, hydrogen

scrubber, gas holder, two compressor units to 30 bar, deoxidizer, and twin tower dryer [29, 62]. Current electrolyzer technology reaches energy efficiencies of 62-82%. The typical current density is 100–400 mA/cm<sup>2</sup> [28, 63]. A large scale electrolysis facility is possible and to date the largest plants can produce about 64 mt of H<sub>2</sub> per day. An added benefit to large scale production is that capital costs decrease per unit energy demand [64]. A standard commercial electrolyzer unit produces 0.09-0.10 kg H<sub>2</sub> and 0.71-0.85 kg O<sub>2</sub> per kg of H<sub>2</sub>O fed [65]. Typical output concentrations are 99.9 to 99.9998% for H<sub>2</sub> and 99.2 to 99.9993% for O<sub>2</sub> [62].

#### **4.3.2 CO<sub>2</sub> Production**

Carbon dioxide is typically thought of as a waste product and emitted into the atmosphere. However as conversion technologies improve efficiencies and yields there are numerous sources of CO<sub>2</sub> for feedstock development. Some of the available sources for CO<sub>2</sub> are fermentation processes such as ethanol production plants, fossil fuel-based power stations, ammonia, cement plants and the atmosphere [45, 66, 67]. The conversion of CO<sub>2</sub> into methanol requires fairly pure CO<sub>2</sub> in order to promote reaction kinetics and avoid catalyst deactivation. A main concern with carbon capture from flue streams (and especially from atmospheric sources) is the low concentration of CO<sub>2</sub> present. While many technologies exist and the process is well studied, carbon dioxide capture is not generally employed on a large scale [45]. Amine solution CO<sub>2</sub> adsorption/desorption systems are the most widely employed to separate CO<sub>2</sub>. However degradation, high energy requirements for solvent recovery and corrosion problems plague these technologies.

To avoid the issues with low CO<sub>2</sub> concentration we have chosen to utilize CO<sub>2</sub> produced by an ethanol fermentation process. Ethanol fermentation is a well-known and extremely old process. The conversion of sugars into ethanol and CO<sub>2</sub> has been around since ancient times. The yeast catalyzed reaction can be seen in equation 24.



Gas outlets from ethanol fermentation contain primarily CO<sub>2</sub> that is saturated with water. Dehydration and compression can then yield nearly pure liquid CO<sub>2</sub> that is ready for transport and use [67].

### 4.3.3 Methanol from CO<sub>2</sub> and H<sub>2</sub>

Methanol production from the hydrogenation of CO<sub>2</sub> progresses in a very similar manner as conventional methanol synthesis. The only difference is rather than a gasification and syngas cleanup steps both CO<sub>2</sub> and H<sub>2</sub> are either provided or produced. As in syngas conversion a Cu/ZnO/Al<sub>2</sub>O<sub>3</sub> catalyst is used for CO<sub>2</sub> hydrogenation to methanol. Typical reactor conditions are 200 – 300 °C and between 15 and 50 bar. Conversion and methanol selectivity is high for the overall process [10]. The reactions of interest are again, CO<sub>2</sub> and CO hydrogenation (equations 21 and 22, respectively) as well as the water gas shift (equation 20).

## 4.4 Materials and Methods

Converting CO<sub>2</sub> into chemicals is thermodynamically challenging, and inherently carries costs for the energy and hydrogen supply [68]. The conversions of reactions 21 and 22 with catalyst of Cu/ZnO/Al<sub>2</sub>O<sub>3</sub> are limited by the chemical equilibrium of the system. The temperature rise must be minimized in order to operate at good equilibrium values. However, selectivity for methanol is high with a value of 99.7% at 5 MPa and 523 K with

a  $\text{H}_2/\text{CO}_2$  ratio of 2.82 [69]. The energy efficiency for the concentrated  $\text{CO}_2$  and hydrogen based methanol is around 46% [68-70].

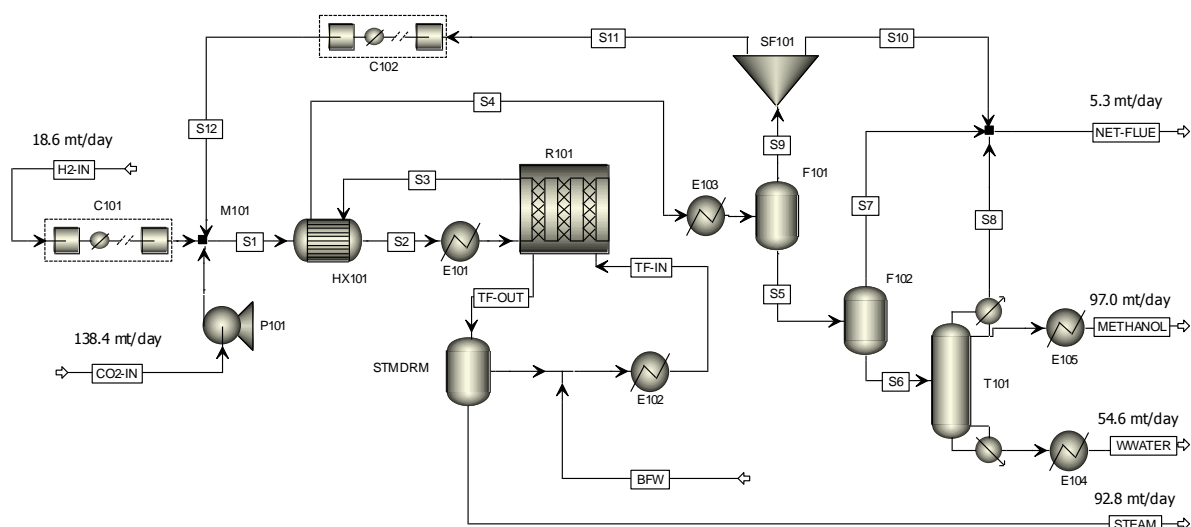


Figure 4.3: Process flow diagram of the methanol plant using a Lurgi reactor and producing steam. [10]

We designed and simulated a methanol plant using Aspen Plus software. Wind-based electrolytic  $\text{H}_2$  and  $\text{CO}_2$  supplied from an ethanol plant are used in the synthesis of methanol. The plant uses 18.6 mt  $\text{H}_2$ /day and 138.4 mt  $\text{CO}_2$ /day, and produces 97.0 mt methanol/day at 99.5 wt% together with 54.6 mt/day of 99.5 wt%  $\text{H}_2\text{O}$  waste water. Figure 4.3 presents the process flow diagram for the methanol plant using  $\text{CO}_2$  and  $\text{H}_2$ . We chose to use the RK-SOAVE property method for estimating the properties of the mixture with gaseous compounds at high temperature and pressure, and the NRTL-RK for the methanol column to better represent the vapor-liquid equilibrium between methanol and water.  $\text{CO}_2$ ,  $\text{H}_2$  and  $\text{CO}$  were defined as Henry's components with this property method. The feedstock is at the conditions associated with typical storage, with  $\text{H}_2$  at 25 °C and 33 bar and  $\text{CO}_2$  at -25.6 °C and 16.422 bar (liquid phase) [28]. The ratio of  $\text{H}_2$  to  $\text{CO}_2$  is held at of 3:1 to promote methanol synthesis. In the feed preparation

block, the renewable H<sub>2</sub> and CO<sub>2</sub> are compressed to 50 bar in a multi-stage compressor and pump, respectively, and mixed with the recycle stream S12 in mixer M101. Stream S1 is preheated in HX101 and E101 before being fed into the plug-flow reactor R101 where the methanol synthesis takes place.

This reactor is representative of the Lurgi's low pressure isothermal reactor [71]. The reactor is simulated as a packed bed reactor with a counter-current thermal fluid. The boiling of the thermal fluid water is used to remove the heat associated with the methanol synthesis reaction. The saturated steam produced (TF-OUT) is fed to a steam drum to produce 92.8 mt/day of steam at 30 bar. The return pressure of the steam drum is used to control reactor temperature and maintains a near isothermal system close to 235 °C. The reactor is a multi-tube reactor using 3900 tubes, each with a diameter 0.07 m and a length of 10 m. These tubes are loaded with a CuO/ZnO/Al<sub>2</sub>O<sub>3</sub> spherical catalyst with a diameter of 5.4 mm, particle density of 1.19 gm/cm<sup>3</sup> and a bed voidage of 0.285 [72]. The reactor operates at 50 bar with pressure drop calculated by the Ergun equation, shown below.

$$\frac{dP}{dz} = 150 \frac{(1 - \varepsilon)^2 \mu v}{\varepsilon^3 \phi^2 d_p^2} + 1.75 \frac{(1 - \varepsilon) \rho v^2}{\varepsilon^3 \phi d_p} \quad 25$$

where  $P$  is the pressure,  $z$  is the reactor length,  $\varepsilon$  is the bed voidage,  $\mu$  is the fluid viscosity,  $v$  is the superficial velocity,  $d_p$  is the particle diameter,  $\phi$  is the particle shape factor and  $\rho$  is the particle density.

Langmuir-Hinshelwood Hougen-Watson (LHHW) kinetics formulations, with fugacities, are used for reactions 21 and 22 while reaction 20 is assumed to be at equilibrium.

LLHW kinetics considers the adsorption of the reactants to the catalytic surface, the

surface reactions to synthesize the methanol and water, and the desorption of the products from the catalytic surface [49]. These formulations can be seen in equations 26 and 27 below.

$$r_{MeOH} = \frac{K_1 f_{CO} f_{H_2}^2 (1 - \beta_1)}{(1 + K_{CO} f_{CO} + K_{CO_2} f_{CO_2} + K_{H_2} f_{H_2})^3} \quad 26$$

$$r_{CO_2} = \frac{K_2 f_{CO_2} f_{H_2}^3 (1 - \beta_2)}{(1 + K_{CO} f_{CO} + K_{CO_2} f_{CO_2} + K_{H_2} f_{H_2})^4} \quad 27$$

where:  $\beta_1 = \frac{f_{MeOH}}{K_{f1} f_{CO} f_{H_2}^2}$ ,  $\beta_2 = \frac{f_{MeOH} f_{H_2O}}{K_{f2} f_{CO_2} f_{H_2}^3}$

$f_i$  is the fugacity of component  $i$ ,  $K_i$  is the kinetic parameter for reaction  $i$ , and  $K_{fi}$  is the equilibrium constant for reaction  $i$  expressed in fugacity. The relevant kinetic parameters can be found in literature [71]. The reactor achieves a single pass conversion of 47% which is similar to that found in literature [72].

The reactor output stream (S3) is fed through HX101 which cools the reactor effluent and preheats the reactor feed. The reactor effluent is further cooled to 25 °C in cooler E103 and fed to flash drum F101. F101 operates adiabatically and at a pressure of 39 bar. This stream is separated into liquid (S5) and gas streams (S9). The gas stream from F101 is sent to a flow splitter SF101, in which 99% of S9 is recycled to the reactor after it is compressed in the compressor C102. Stream S5 is fed to another flash drum, F102, to further remove dissolved gasses from the crude methanol. F102 operates adiabatically at atmospheric pressure. The crude methanol is separated from the water in the distillation tower T101. The product methanol is the distillate, while the wastewater is the bottoms flow of T101. The column has 20 stages with sieve trays, the feed (S6) enters at stage 15.



The column has a partial condenser that cools the distillate stream to 55 °C; this removes most of the residual CO<sub>2</sub>. The gaseous CO<sub>2</sub> in stream S8 is mixed with the gas stream (S7) from F102 and the recycled bleed and vented to the atmosphere. The NET-FLUE stream contains mostly CO<sub>2</sub> with less than 0.5% of the produced methanol being lost. The mass fraction of methanol in the distillate and bottoms is controlled by varying the reflux ratio and the ratio of bottoms flow to feed flow rate (B:F). This was done by using two design specifications in the Radfrac column T101. Column specifications and operating conditions can be found in Table 4.1: Column specifications and results for column T101.

*Table 4.1: Column specifications and results for column T101 [10]*

Column T101 specification/results	Value
Stages	20
Feed stage	15
Height (m)	20
Diameter (m)	1.16
Reflux ratio (molar)	0.959
B:F* (molar)	0.498
Condenser temp (°C)	55

\*B:F Bottom flow to feed ratio

The waste water stream and product methanol are cooled by the heat exchangers E104 and E105, respectively. The methanol and wastewater are then stored. Table B2 in the Appendix B shows the properties of input and output streams of the methanol plant. Methanol production has the potential for the best possible technology deployment ranging from 16% to 35% [68]. Therefore, the design reflects that potential in a simple design delivering almost pure methanol and waste water containing less than 1% methanol. Steam is a valuable byproduct of this system producing roughly 1 mt of steam/mt of methanol. Utilization of this steam leads to a high thermal efficiency of this process. Common practice is to use the steam to produce electricity to power the

compressors and pumps, while any residual steam can then be used as process heat. Another option is to use the saturated steam produced (TF-OUT) to preheat the reactor input from inlet conditions (-14 °C) to reactor operating conditions (235 °C). The reactor effluent would then be used to preheat the distillation column feed to the feed stage temperature. Both of these designs of steam use and heat integration represent energy efficient methods of methanol production from renewable inputs.

The separation section uses an optimized process using one column for methanol distillation. While gas removal and heat integration could be accomplished by using multiple columns [73] the additional capital and operating costs associated with multiple columns could make the process less economically feasible. This work represents a practical example of methanol production using kinetics based on experimental data using a commercially available catalyst [71]. However, future work to improve the process could be conducted including; heat integration between the H<sub>2</sub> and CO<sub>2</sub> production plants and in the methanol process itself, further column optimization using Aspen Plus column targeting tools, optimization of recycle flash drums to minimize the duty of C102 while increasing CO<sub>2</sub> recycle and scale up considerations (Lurgi's two reactor concept) for the production of larger quantities of methanol [72, 73].

## **4.5 Results**

### **4.5.1 Sustainability**

The integral methanol production facility consists of an electrolytic hydrogen production unit, CO<sub>2</sub> capture and storage unit, and the methanol production unit as shown in Figure 4.4.

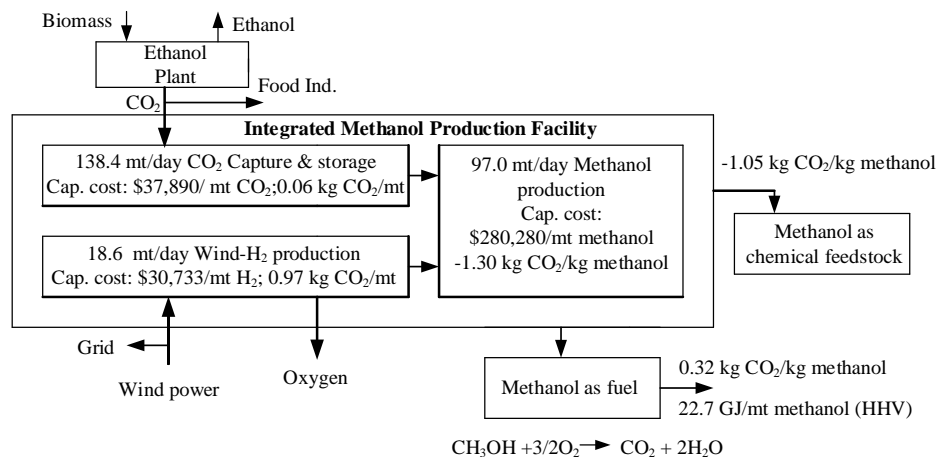


Figure 4.4: Some economic and sustainability indicators in the integral methanol production facility. [10]

Table 4.2 shows the sustainability indicators of the integral methanol plant. The facility requires 18.56 mt H<sub>2</sub>/day and 138.37 mt CO<sub>2</sub>/day in total and produces 97.0 mt methanol/day and 148.39 mt O<sub>2</sub>/day. The total emissions of CO<sub>2</sub> from are 18.01mt CO<sub>2</sub>/day for the H<sub>2</sub> production and 6.10 mt CO<sub>2</sub>/day for the CO<sub>2</sub> capture and storage. The methanol production plant reduces emissions by -118.41 mt CO<sub>2</sub>/day if the steam produces electricity or by -126.38 mt CO<sub>2</sub>/day if the steam is used as process heat.

Table 4.2: Sustainability indicators for the integral methanol plant\* [10]

<b>Material indicators</b>	<b>Integral methanol production</b>			
	MeOH Prod. (a)	MeOH Prod. (b)	H <sub>2</sub> Prod.	CO <sub>2</sub> C&S
CO <sub>2</sub> production, mt/day				138.37
H <sub>2</sub> production, mt/day			18.56	
Methanol production, mt/day	97.01	97.01		
Oxygen production, mt/day			148.39	
<b>Energy intensity indicators</b>				
Total heating/electricity duty, MW	2.38	1.14	41.34	1.26
Total cooling duty, MW	5.79	5.39	0.12	0.06
Net duty (heating - cooling), MW	-3.42	-4.25	41.22	1.20
Total heating cost, \$/h	24.60	31.05	3204.11	97.81
Total cooling cost, \$/h	4.42	4.12	0.09	0.04
Total cost (heating + cooling), \$/h	29.02	35.17	3204.20	97.85
<b>Environmental impact indicators</b>				
Net stream CO <sub>2e</sub> , mt/day	-133.66	-133.66	0.00	0.00
Utility CO <sub>2e</sub> , mt/day	15.25	7.28	18.01	6.10
Total CO <sub>2e</sub> , mt/day	-118.41	-126.38	18.01	6.10
Net carbon fee, \$/h	-9.87	-10.53	1.50	0.51

\*US-EPA-Rule E9-5711; natural gas; carbon fee: \$2/mt.

(a) Methanol production producing steam

(b) Methanol production utilizing steam as heat

Table 4.2 shows the main results of the material and energy usages, as well as the CO<sub>2</sub> emissions for the integral facility. The reductions in the net carbon fee range between -\$9.87 and -\$10.53 for the methanol facility depending on how the steam is utilized. This is based on a set value of \$2/mt CO<sub>2e</sub>. As Table 4.2 shows, the values of total duty and cost are the highest for the hydrogen production unit used in the methanol production.

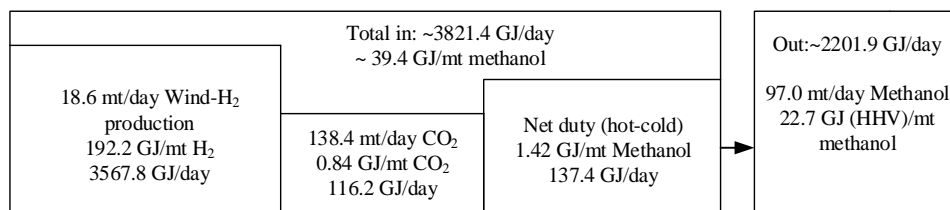


Figure 4.5: Overall energy balance for the integral methanol production facility. [10]

Figure 4.5 presents an approximate energy balance with the energy required at the electrolyzer, for carbon capture and storage, and total duty required in methanol production versus energy content in methanol as fuel combusted fully. The energy efficiency for the integral facility for both steam utilization routes is around 57.6%. This is in line with the results shown in Mignard et al. [51] who showed efficiencies ranging from 51 to 58%. A comparison to the literature values the energy efficiency of this process is comparative with coal and biomass based syngas processes [68, 70].

*Table 4.3: Sustainability metrics for the integral methanol plant, with steam production (a) and with steam utilization (b) [10]*

Material Metrics	(a)	(b)
CO <sub>2</sub> used/Unit product	1.43	1.43
H <sub>2</sub> used/Unit product	0.19	0.19
Energy intensity metrics		
Net duty/unit product, MWh/mt	0.40	0.39
Net cost/Unit product, \$/mt	824.09	825.61
Environmental impact metrics		
Total CO <sub>2</sub> e/Unit product	-0.97	-1.05
Net carbon fee/Unit product, \$/mt	-1.94	-2.11

\*US-EPA-Rule E9-5711; natural gas; carbon fee: \$2/mt.

Table 4.3 presents the sustainability metrics for the integral methanol plant in which the indicators are normalized with respect to the amount of methanol produced. The material intensity metrics show that the methanol facility requires 1.43 mt CO<sub>2</sub>/mt methanol. The energy intensity metrics favors when steam is used to produce electricity, with the net utility cost around \$824.09/mt methanol. The environmental impact metrics show that the integral methanol facility with heat utilization of steam reduces emission by around -1.05 kg CO<sub>2</sub>/kg methanol when utilizing it as a chemical feedstock for CO<sub>2</sub> fixation (e.g. formaldehyde, acetic acid, methyl methacrylate, etc.) and recycles 0.32 kg CO<sub>2</sub>/kg

methanol after its complete combustion when used as a fuel/fuel additive, as seen in Figure 4.4.

#### 4.5.2 Economic Analysis

The economic analysis of the integral methanol plant is based on the discounted cash flow diagrams (DCFD) prepared for ten-years of operation using the current technology and economic data. An example calculation of a DCFD is shown in Appendix B. Based on the equipment list from the process flow diagram (Figure 4.3), bare module costs are estimated and used as fixed capital investments (FCI). Chemical Engineering Plant Cost Index (CEPCI-2014) (= 576.1) [74] is used to estimate and update the costs and capacity to the present date by

$$Cost_{new} = Cost_{old} \frac{CEPCI_{new}}{CEPCI_{old}} \left( \frac{Capacity_{new}}{Capacity_{old}} \right)^x \quad 28$$

where  $x$  is the factor, which is usually assumed to be 0.6. Working capital is 20% of the FCI. Depreciation method is the Maximum Accelerated Cost Recovery System (MACRS) with a 7-year recovery period [75]. After estimating the revenue and the cost of production, DCFD is prepared to estimate the three economic feasibility criteria that are Net Present Value (NPV), Payback Period (PBP), and Rate of Return (ROR). In addition, the economic constraint (EC) and the unit product cost (PC) are also estimated by

$$EC = \frac{\text{Average Discounted Annual Cost of Production}}{\text{Average Discounted Annual Revenue}} \quad (29)$$

$$PC = \frac{\text{Average Discounted Annual Cost of Production}}{\text{Capacity of the Plant}} \quad (30)$$

The PC takes into account the operating and maintenance (O&M) costs. An operation with  $EC < 1$  shows a more feasible operation with the opportunity to accommodate other costs and improve the cash flows toward more positive NPV. The calculations of average discounted annual cost of production, average discounted annual revenue, and capacity of the plant are given in the Appendix equations; B1, B2, and B3, respectively.

At the current capacities, the estimated approximate values of the FCIs are \$5.87 million for the wind-based electrolytic H<sub>2</sub> production unit, \$4.52 million for the CO<sub>2</sub> production unit, and \$28.13 million for the methanol production unit. The H<sub>2</sub> production includes the compression, storage, and dispensing from a centralized production facility with an average electricity cost of 0.045/kWh. Therefore, the total value of the FCI for the integral methanol plant is around \$38.52 million.

The distribution of unit capital costs for the integral methanol production facility shows that the contribution from wind-based H<sub>2</sub> is the highest (Figure 4.4). The production cost of H<sub>2</sub>, which makes the NPV = 0, is \$1.37/kg H<sub>2</sub> when the selling price of methanol is \$600/mt with the corresponding values of  $EC = 0.87 (< 1)$  and  $PC = 658.25/\text{mt}$  methanol ( $> \$600/\text{mt}$ ). Global prices of methanol change widely; the prices as of July 2015 are \$403/mt in Europe, \$442/mt in North America, \$375/mt and in Asia Pacific [42].

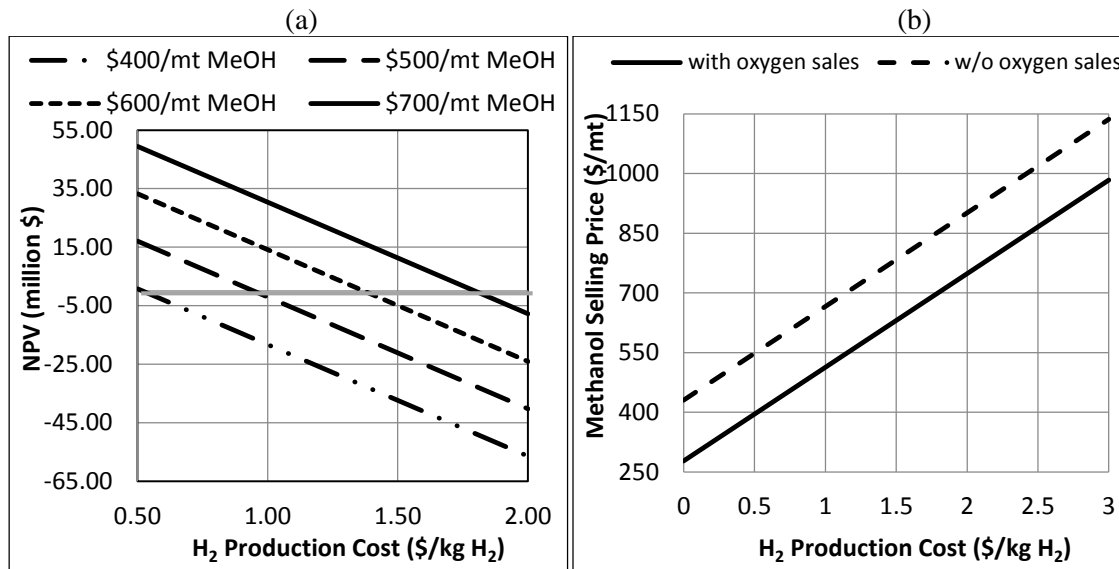


Figure 4.6: The influence of H<sub>2</sub> production cost on: (a) net present value at constant methanol (MeOH) price, (b) Selling price of methanol for NPV = 0 with and without selling O<sub>2</sub> byproduct at \$100/mt. [10]

The cost of renewable hydrogen and the selling price of methanol affect the economics of the renewable methanol. We have evaluated the final NPV for varying methanol prices and hydrogen prices, the results can be seen in Figure 4.6a. The minimum selling price of methanol was also investigated with varying hydrogen production cost (seen Figure 4.6b). This is the selling price of methanol that makes the NPV = 0 after 10 years. The inclusion and exclusion of O<sub>2</sub> sales was also investigated in Figure 4.6b. A summary of the minimum selling price of methanol versus H<sub>2</sub> production cost can be seen in

Table 4.4.



Table 4.4: Effect of methanol selling price on the maximum unit production cost of renewable hydrogen (NPV = 0 after 10 years). [10]

MeOH Price (\$/mt)	H <sub>2</sub> cost (\$/kg)	EC (\$/\$)	PC (\$/mt)
375.00	0.41	0.817	432.21
403.00	0.53	0.827	460.45
442.00	0.70	0.838	498.11
512.82	1.00	0.855	571.09
630.50	1.50	0.877	688.75
748.18	2.00	0.893	806.43
983.54	3.00	0.915	1041.79

The general trends in these graphs indicate that a higher selling price for methanol raises the cost of hydrogen at which the process becomes feasible (NPV > 0). It also indicates that the sale of the O<sub>2</sub> byproduct could be crucial to the economic feasibility of the process. The price of methanol at the DOE's targeted production cost of \$2/kg H<sub>2</sub> [76, 77] is higher than current pricing of methanol. However, methanol pricing is in the ballpark of current rates using the IEA's target of \$0.30/kg H<sub>2</sub> [68, 78].

Renewable hydrogen-based methanol would recycle carbon dioxide as a possible alternative fuel to diminishing oil and gas resources [79]. There are already vehicles which can run with M85, a fuel mixture of 85% methanol and 15% gasoline [23, 45]. Methanol can be used with the existing distribution infrastructure of conventional liquid transportation fuels. In addition, fuel cell-powered vehicles are also in a fast developing

stage, although they are not yet available commercially [23, 24, 80]. Technological advances such as these would lead to a “methanol economy” [28, 45, 20-82].

#### **4.5.3 Multi-Criteria Decision Matrix**

Beside the economic analysis, sustainability metrics should also be used to evaluate the feasibility of chemical processes [83, 84]. For this purpose, Table 9 shows a multi-criteria Pugh decision matrix [85] to assess the renewable and nonrenewable methanol production facilities. Also shown in this figure is a comparative analysis for renewable ammonia and fossil-based ammonia. Ammonia is included because of its use of renewable hydrogen as a chemical feedstock. Explanation of this work can be found in our published work [86]. This highlights the use of this decision matrix for both fuels/energy production and chemical processing. The matrix generates the number of plus, minus, overall total, and overall weighted total scores. The weighted total adds up the scores times their respective weighting factors. The weight factors can be adjusted with respect to the location, energy policies, and energy costs and security. The totals are guidance only for decision making. If the two top scores are very close, then they should be examined more closely to make a more informed decision. Renewable energy-based systems may require the combined use of scenario building and participatory multi-criteria analysis for sustainability assessment [84].

With the weight factors adapted and the combined economic and sustainability indicators, the decision matrix in Table 4.5 shows that overall weighted score is around +5.4 for the renewable integral methanol facility, which is higher than that of fossil fuel based methanol. It should be noted that the weighting factors shown in this table are subjective and will vary depending on the needs determined by the matrix user. This will change the

overall weighted score however the total plus/minus values will remain largely unchanged. The use of this table however may display the impact of sustainability indicators on evaluating the feasibility of chemical processes requiring large investments and energy resources.

Table 4.5: Multi-criteria decision matrix for feasibility assessment of chemical processes and energy systems. [86]

Economics and sustainability indicators	Weighting factor:0-1	Fossil-methanol	Non-fossil-methanol	Fossil-ammonia	Non-fossil-ammonia
<b>Economic indicators</b>					
Net present value NPV	1	+	-	+	-
Payback period PBP	0.8	+	-	+	-
Rate of return ROR	0.8	+	-	+	-
Economic constraint EC	0.9	+	-	+	-
Impact on employment	1	+	+	+	+
Impact on customers	1	+	+	+	+
Impact on economy	1	+	+	+	+
Impact on utility	0.7	-	+	-	+
<b>Sustainability indicators</b>					
Material intensity	0.7	-	+	-	+
Energy intensity	0.8	+	-	+	-
Environmental impact GHG in production	0.8	-	+	-	+
Environmental impact GHG in utilization	0.8	-	-	+	+
Toxic/waste material emissions Process safety and Public safety	1	-	+	-	-
Potential for technological improvements and cost reduction	0.8	-	+	-	+
Security/reliability	0.9	-	+	-	+
Political stability and legitimacy	0.8	-	+	-	+
Quality of life	0.8	-	+	-	+
Total positive score		8	11	9	11
Total minus score		9	-6	-8	-6
Net score (positive-minus)		-1	+5	+1	+5
<b>Weighted total score</b>		<b>+0.2</b>	<b>+5.4</b>	<b>+2</b>	<b>+4</b>

## 4.6 Conclusions

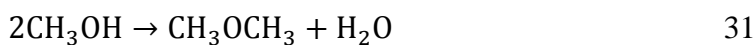
Use of wind energy-based hydrogen and CO<sub>2</sub> for methanol synthesis may lead to the reduction in carbon emissions either by recycling and/or fixation. The cost of renewable hydrogen production plays an important role within the economics and determines the scope of technological improvements for electrolytic hydrogen-based methanol production. With current methanol prices hydrogen production costs are required to be between \$0.40 to \$0.70/kg of H<sub>2</sub>, for the NPV = 0. More research is required in electrolysis technologies to reduce hydrogen production cost. However, we have shown the sale of product oxygen from electrolysis could play an important role in improving economic feasibility. Further work is needed for identifying possible low cost back-end processes that could convert the product methanol into value added chemicals. A life cycle assessment of these chemicals could be conducted to show how much of the CO<sub>2</sub> is ultimately fixed and the overall sustainability of the process. Additionally, further improvements in process integration for hydrogen and CO<sub>2</sub> supply into methanol synthesis would have a positive impact of hydrogen and methanol economies. A multi-criteria decision matrix, containing the economics and sustainability indicators, has been introduced for a more comprehensive feasibility assessment. This matrix may help account for the cost of environmental damage from using fossil fuels in the overall assessment of feasibility. It also shows that although chemical processes using non-fossil fuels may be limited economically these more environmentally conscious processes may achieve better overall assessment scores. This is in line with the need for a better assessment of chemical processes and energy technologies in order to address the

sustainability within the context of global challenges of energy security, climate change, and technological advancement.

## CHAPTER 5 CHEMICAL PROCESS INDUSTRIES – DIMETHYL ETHER PRODUCTION

### 5.1 Introduction

Dimethyl ether has recently gained attention for its potential use as an alternative transportation fuel. DME has a higher cetane number than diesel (55-60 versus 40-55 for diesel) and its combustion also results in lower NO<sub>x</sub> and SO<sub>x</sub> emissions. While DME is a volatile organic compound (VOC) it is non-toxic, non-carcinogenic, non-teratogenic and non-mutagenic. It has also been shown to be environmentally benign [87]. Direct fuel use of DME would require some modifications to current infrastructure as it requires pressurization. However, the minor modifications that would be required would be based on existing infrastructure and would be cheaper than building from the ground up [88]. There exist two methods of dimethyl ether production, direct and indirect. The indirect method first involves the production of methanol and then further catalytic dehydration of this methanol into dimethyl ether (equation 2).



The direct method combines these two steps into one reactor and produces dimethyl ether directly from syngas. The avoidance of methanol purification and an extra reactor make direct conversion economically and thermodynamically favorable over indirect methods. However these technologies suffer from low selectivities and are still in their industrial infancy [89, 88].

The indirect method of DME production can be seen as an additional backend process to methanol production. It can handle any of the feedstocks or methanol production technologies that give reasonably pure methanol as an output. The DME formation

reaction occurs in a gas phase fixed bed reactor over a  $\gamma$ -Al<sub>2</sub>O<sub>3</sub> catalyst. Operating conditions are around 250 – 400 °C and 10 – 25 bar [88]. High methanol conversions (80% - 90%) and DME selectivities (~99.9%) are typically observed [90]. A series of purification steps are taken after the reactor. Pressurized columns are the norm as the low boiling point of DME causes difficulties with atmospheric separation.

Identifying the environmental impact fuels may have on the environment is tough because the use of these fuels inherently effects the environment. As well many fuels utilize fossil fuel-based raw materials. The use of life-cycle assessment in monitoring fuel impacts is crucial. LCA allows direct comparisons between the total environmental burdens distinct fuels can have. This chapter focusses on a life-cycle assessment of two alternative fuels; methanol and dimethyl ether. Methanol is produced as described in Chapter 3 and DME is produced as a back-end process to this methanol facility. A full comparative LCA is performed between these fuels and conventional fuels.

A number of articles have been published based on the life cycle analysis of methanol production. However, the renewable based processes mainly focus on gasification of biomass as the ultimate chemical feedstock. A substantial review of current literature work can be found in Quek et al. [91]; some relevant papers will be discussed here. Renó et al. [92, 93] has published two papers relating the environmental impacts of methanol production from sugarcane bagasse using a life cycle assessment. Their work provides a detailed estimation of biomass to liquid technology and a comparison to other methanol technologies. They also introduce an integration scheme between ethanol and methanol plants both using sugarcane. The close proximity of the plants allows an ethanol cogeneration system to provide process heat and electricity to the methanol production

facility. The integration of ethanol and methanol processes reduces fossil energy demand and environmental impacts while increasing biofuel production diversity. A life cycle greenhouse gas emissions study for methanol production from biomass gasification is discussed in Holmgren et al. [94]. Again integration between industrial sectors is cited to have greater potential for reducing GHG emissions. Many different integration schemes were investigated in their work and methanol conversion (to olefins) was also addressed. Wu et al. [95] conducted a well-to-wheels investigation into using switchgrass to produce liquid fuels. Aspen Plus was used to model biofuels production and GREET was used to estimate environmental impacts. The biomass based fuels were able to reduce fossil energy consumption 65-88% (per mile basis) as well as reduce greenhouse gas emissions 82-87%.

Dimethyl ether was one biofuel addressed in the work by Wu et al. There are a number of studies conducted on life cycle assessment of dimethyl ether production. An extensive report on DME production, use and life cycle can be found in work prepared by the University of California Davis and Berkeley [96]. Renewable DME (produced by  $\text{CH}_4$  from anaerobic waste digestion) is compared to natural gas based DME and ultra-low sulfur diesel. A variety of biomass feedstocks and their influence on DME production are analyzed in work by Higo and Dowaki [97]. Again, gasification is the method of biomass conversion addressed in their work. A well-to-wheels assessment is provided in Semelsberger et al. [87] that highlights environmental impact of DME production from natural gas to a variety of other fuels and feedstocks. Together, renewable methanol and DME show exciting promise in the light of sustainability of processes and feasibility.



## 5.2 Materials and Methods

### 5.2.1 Dimethyl Ether Simulation

From our point of view indirect dimethyl ether synthesis is no more than a backend conversion process for a methanol facility. The production of DME from methanol follows the simple dehydration reaction between two methanol molecules (Equation 31). This reaction is usually catalyzed by alumina based catalysts [98]. A fixed bed reactor packed with catalyst is usually employed industrially. Typical reactor temperatures are around 250 - 400 °C while pressure values can vary from 10 to 25 bar. At these conditions methanol conversions can approach 70-85%, nearing equilibrium values. Selectivity is also usually high with a small amount of formaldehyde being produced [88, 99, 100].

We modeled DME production in Aspen Plus using a continuation of the methanol process described in previous work [10]. The process utilizes 96.2 mt/day of methanol and produces 67.8 mt/day of 99.6 wt% DME. This simulation uses the NRTL-RK property method to properly model vapor-liquid equilibrium between methanol, water and dimethyl ether. The DME process flow diagram can be seen in Figure 5.1. The methanol production facility is encapsulated in the MEOHPROD block; this hierarchy block contains the full process flow diagram produced in our previous work. The remainder of the process flow diagram is associated with DME production.

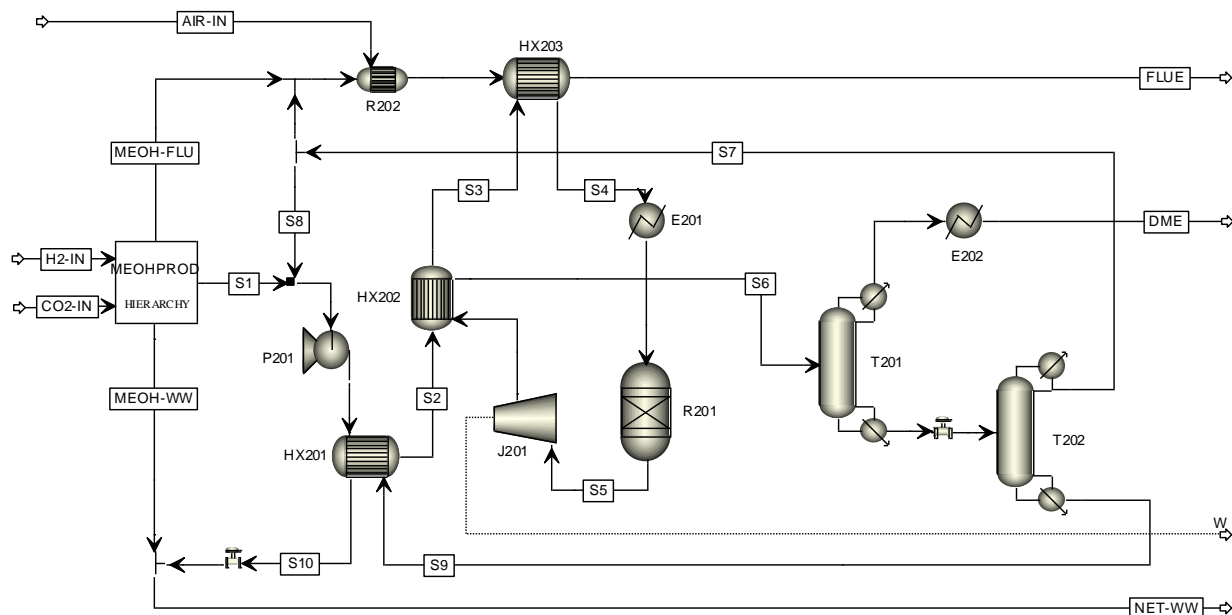


Figure 5.1: Process flow diagram for the backend DME facility

The product methanol (S1) is first mixed with a recycle stream (S8) containing unreacted methanol separated in column T202. This stream is then brought up to reactor conditions with a pump (P201) and a series of heat exchangers. The heat exchangers capture process heat from the waste water stream (HX201), from the reactor effluent (HX202) and the combusted flue gas (HX203). The heat exchangers are modeled as fixed tube shell and tube heat exchangers. Associated parameters for all of the heat exchangers can be seen in

Table 5.1. A rigorous modeling approach was taken in modeling these heat exchangers which calculates the pressure drop for both streams. High pressure steam is used to bring the stream to final conditions of 17 bar and 275 °C in E201.

Table 5.1: Operating conditions and results for the three heat exchangers

	HX201	HX202	HX203
Specified UA ( $cal/s K$ )	471.12	1695.21	335.4
Specified area ( $m^2$ )	2.05	4.19	6.78
Heat Transfer (kW)	117	378	338

The reactor (R101) is modeled as an RGIBBS reactor which calculates the minimum free energy of the products at the specified temperature and pressure. The choice of this reactor assumes that the reaction reaches equilibrium at these operating conditions. A sensitivity analysis was run to ensure consistent conversions and selectivities with literature data [88]. The effluent contains an equilibrium mixture of methanol, dimethyl ether, formaldehyde and water. Methanol conversion reaches 87.2% while selectivity to DME is 99.5%.

The effluent is brought down to 10 bar in a turbine (J201) to recover energy from this stream before product separation. The turbine collects 71.8 kW of energy which can help power the reactor feed pump. After the turbine, the reactor effluent is cooled in HX202 and fed to the first distillation column. The first column separates out the product DME. It operates at 9.5 bar to facilitate DME separation while maintaining an achievable condenser temperature. Lower pressure columns result in negative condenser temps which cannot feasibly be done. Internal column design specifications were set so that the vapor distillate reaches a purity of 99.6 wt% DME and the column recovers 99% of the

DME in this stream. This was done by varying the reflux ratio and the distillate to feed ratio. The product DME stream is cooled to 30 °C in E202 which liquefies the compressed DME for transport and sale.

The bottoms is fed to a second column (T202) to recover unreacted methanol. This column operates at 7 bar. The methanol recovered in the distillate is sent back to the beginning of the process. Some of this stream (0.5 mol %) is bled and mixed with the flue stream from the methanol facility. The bottoms is mixed with the waste water from the methanol facility and sent for conditioning. We have assumed that this waste treatment step reduces the formaldehyde concentration to 0.1%. The design specs for column T202 were set to recover 99.5% of H<sub>2</sub>O in the bottoms and 95% of the methanol in the distillate. As in column T201, the reflux ratio and distillate to feed ratio were varied to accomplish this. Column operating conditions and specifications for both columns can be seen in Table 5.2.

*Table 5.2: Column specifications and results for the DME process towers*

Column specifications/results	T201	T202
Pressure (bar)	9.5	7
Stages	15	25
Feed stage	6	17
Height (m)	10.5	17.5
Diameter (m)	0.66	0.7
Reflux Ratio (molar)	3.30	1.94
D:F* (molar)	0.43	0.22

\*D:F = Distillate to Feed ratio

The combined flue streams are mixed with a fresh air supply and combusted in a thermal oxidizer, R202. This is done to prevent the emission of volatile organic compounds and has an added benefit of recovering some process heat. The combustion is simulated in

R202 which is modeled as another RGIBBS reactor operating adiabatically and at atmospheric pressure. This succeeds in removing all of the methanol and DME from the flue gas. The gas exits at a temperature of 800 °C and is sent to HX203 to further preheat the reactor feed. A full stream table of input and output streams can be found in the Appendix.

The first step in a life-cycle assessment is the establishment of a system boundary. It is important to clarify what we wish to study as well as the depth that we want to consider. It is clear that we wish to investigate the impact of methanol production from CO<sub>2</sub> and H<sub>2</sub>. We know that the CO<sub>2</sub> will be produced from biomass fermentation and that the H<sub>2</sub> will be supplied by wind powered water electrolysis. We also want to investigate the conversion of this methanol into other fuels (DME) or its direct use as a fuel. By tracing process inputs back to their source and investigating the required raw materials for these steps we can establish an LCA map (Figure 5.2)

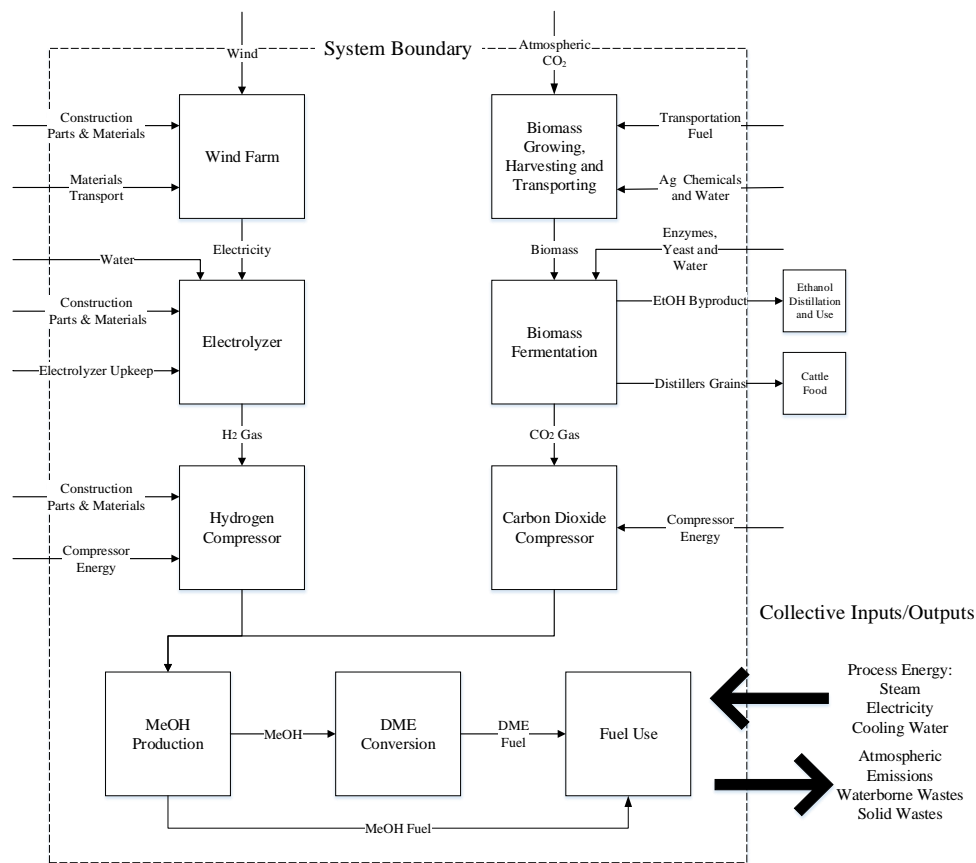


Figure 5.2: A map detailing the system boundary of the LCA and the inputs/outputs and processes we are investigating.

This full map will be broken into pieces and individually addressed in subsequent sections. Data that was not produced in the simulations above was gathered via literature search of published data or found using provided GREET simulations.

## 5.2.2 Life-Cycle Assessment

### 5.2.2.1 H<sub>2</sub> Production

We have assumed that we will use an electrolyzer operating at atmospheric conditions with power requirements and production rates found in literature. We have assumed a single electrolyzer can operate at a H<sub>2</sub> flow rate of 485 Nm<sup>3</sup>/hr and would require 4.1 kWh/Nm<sup>3</sup> [30]. A single large scale industrial electrolyzer maxes out around these

production values. In order to produce methanol at the quantity specified above we would require 18 of these large electrolyzers operating together in series. As well, the energy demand to power this array of electrolyzers is around 35.8 MW which would require 12, 3 MW turbines for complete operation.

The environmental emissions and inputs for the wind-based electrolysis section of this plant were produced using GREET software and data attained from an extensive literature search. Spath and Mann [101] have presented a detailed report on the total life cycle analysis of hydrogen production via wind-based electrolysis. They show the influence of the manufacture, transport and installation of wind turbines as well as electrolysis and compression/storage. These aspects represent the major technologies that go into the production of electrolytic hydrogen and are what our LCA on wind-based H<sub>2</sub> will be focused on.

The manufacture of a wind turbine starts with the production of its individual components; the tower, generator, gearbox, nacelle, rotor and blades. These components are then shipped to the final location and installed. Installation requires the pouring of a reinforced concrete foundation. Materials required for the production of a 3 MW, horizontal axis, 3 blade wind turbine were found in literature [102]. While materials are known, individual production techniques and associated emissions are site specific and typically considered small enough to be irrelevant [103]. It is also important to note that the decommissioning of these wind turbines is not addressed in this assessment.

The individual components were submitted into the GREET system along with their materials of construction. Shipment from production facilities was also simulated, using transport data found in literature [104]. We have assumed the model 2 suppliers in the

associated literature and assumed these turbines would be located in southeast Nebraska. A collection of transport data can be found in Appendix C. The transport of individual components to the central facility was also simulated in GREET. We assumed heavy-duty trucks would be used to transport the pieces of the turbines. At this stage the addition of a reinforced concrete foundation [102] was also implemented. The assembly of the turbine was assumed to have a negligible effect on analysis. The turbines were assumed to have a net annual output of 29,743 MWh and to operate for 20 years [102]. The environmental outputs from the simulation were normalized to a functional unit of MWh based on the turbines total life. The emissions for the production of electricity for electrolysis was calculated based on these normalized values and attributed to the turbine section of the assessment.

Data for the components of an electrolyzer were found in literature [65]. We have chosen to investigate the production of the electrolyzer and compressor units and their maintenance requirements in the scope of this LCA. The literature values were taken and entered into the GREET platform to establish emissions and material requirements. We have assumed that transportation is of negligible importance when compared to production and use costs of the electrolyzer [101]. The energy required to compress the production hydrogen from the outlet conditions to 30 bar was calculated in Aspen Plus and used as an input for the “Electrolyzer Use” process in the GREET simulation. The results of all the hydrogen production steps were compiled and use the functional unit of 1 mt of H<sub>2</sub>.



### 5.2.2.2 CO<sub>2</sub> Production

CO<sub>2</sub> is produced as a byproduct of the fermentation of sugars into ethanol. Ethanol production is a widely studied technology in GREET due to its nationwide use as a fuel. However, to date CO<sub>2</sub> is not seen as a byproduct of ethanol production [105]. By converting this waste product into a valuable commodity we could improve the economic viability of ethanol production. As our main focus is the byproduct CO<sub>2</sub> we have chosen to forgo a full analysis into the production of ethanol and to use data provided by the GREET database. Due its industrial maturity, we have chosen to base our analysis on a dry milling, corn ethanol production facility. The total ethanol process includes corn farming, corn transportation to the plant and then ethanol production. A brief description of this process will be described below however a more detailed description can be found in literature [106].

The GREET model for corn farming includes; production of fertilizers (e.g. NH<sub>3</sub>, urea, K<sub>2</sub>O, P<sub>2</sub>O<sub>5</sub>, CaCO<sub>3</sub>, etc.), pesticides, herbicides, water use, and fossil energy (required for farm equipment, kernel drying, water pumping, etc.). All of these inputs are added in proportion to the output corn amount according to current farming statistics [107].

Transportation includes shipment by truck from farm to distribution facility and ultimately to the bio-refinery. The ethanol production facility takes in this corn along with additional alpha and gluco amylase, yeast and water. The process requires fossil fuel inputs of coal, natural gas, and electricity. For every one gallon of ethanol produced 2.556 kg of distiller grains and solubles (DGS) and 3.08 kg of CO<sub>2</sub> are produced. The amount of DGS was provided in the GREET analysis while the value for CO<sub>2</sub> was found in literature [108]. The produced ethanol and DGS are then shipped but this is beyond the scope of our LCA.

As ethanol is the main product of the fermentation process we must determine how to fairly assign the emissions between ethanol and the byproducts. As we focus on the further conversion of CO<sub>2</sub> into value added products we must assume that CO<sub>2</sub> has an economic value. This allows us to use economic allocation to assess the environmental impacts of CO<sub>2</sub> production from the ethanol process [109]. Assuming a value of \$40/mt CO<sub>2</sub> [110], \$1.43/gal ethanol [111] and \$180/mt DGS [112] we can create an allocation factor to scale the results to account for the different co-products that are produced. These calculations can be seen in Appendix C.

The total well-to-product emissions for ethanol production are scaled by multiplication by the allocation factor. This effectively allocates the emissions to the byproduct CO<sub>2</sub> according to the economic value it has compared to the other products.

The requirements for compression were taken from literature [67]. This source accounts for compression and water removal from fermentation based CO<sub>2</sub>. The CO<sub>2</sub> stream out of the fermenter is nearly pure (~96 mol%) and at atmospheric conditions with a temperature of 27 °C. The stream leaves the compression stage as liquefied CO<sub>2</sub> at 16.4 bar. The electricity requirement was entered into the GREET platform to determine the environmental impacts for the compression stage. This data was then compiled with the other CO<sub>2</sub> capture and compression data, normalized to the production of 1 metric ton of CO<sub>2</sub>. Emissions data was not calculated for the production of the unit operations for the CO<sub>2</sub> compression as the utility requirements over the life time of the plant largely outweigh the impact their production generates [113].

### 5.2.2.3 Methanol/DME Production

Methanol and DME production facilities were simulated in Aspen Plus. The data concerning direct CO<sub>2</sub> emissions and utilities use were taken from these simulations. Important utilities data for these simulations can be seen in Table 5.3. This data was taken directly from the ASPEN interface and assume the ultimate energy source as natural gas.

Table 5.3: Unit energy cost for various utilities with energy source of natural gas for 2014 [22]

Utilities	Energy price, \$/MJ	$T_{in}$ °C	$T_{out}$ °C	$U^*$ kW/m <sup>2</sup> K
Electricity	\$0.0775/kW h			
Cooling Water	\$0.09/mt	20	25	3.75
Steam (HP)	$2.5 \times 10^{-3}$	250	249	6.00

\* Utility side film coefficient for energy analysis.

The total steam and electrical energy required for the plants were calculated in ASPEN. This value was taken and implemented in the GREET model for steam production using natural gas as a fuel. Electricity required for the facility is assumed to come from the wind turbines and the emissions on an energy basis were used to calculate the electricity demand data. Direct CO<sub>2</sub> emissions in the flue gas of the plants were also added to the utility emissions data to provide a complete analysis.

We have also collected data for product storage and transportation to fueling stations as would be required for the use of these products as fuels. The data for this is built into the GREET software. The data estimated for methanol/DME production and transportation were normalized on a per mt product basis. That is, data was compiled using 1 mt of methanol or 1 mt of DME as the functional unit for the methanol and DME plants, respectively.

Conventional production of methanol and DME were also investigated using the GREET software. Raw materials, transport, production and distribution are all accounted for in these simulations. The only change made was an erroneous data value for CO<sub>2</sub> emissions in the DME production pathway. The original negative value was converted to 23,158 g/mmbtu which was taken from a report compiled by Argonne [114].

#### **5.2.2.4 Fuel Utilization**

GREET analysis also allows us to investigate the utilization of different fuels in a variety of different vehicles. A comparison between our renewably based methanol and dimethyl ether was made to conventional (fossil fuel based) methanol and dimethyl ether. The data collected for the conventional processes was taken from the GREET platform. Using this method we were able to detail the emissions and energy from utilizing the fuel in order to more directly compare methanol and DME on a per energy basis. With this we were able to compare the results of our simulations to conventional methanol and DME production routes as well as other renewable production methods. Three simulations were compared in all, two renewable options and one based on natural gas feedstock. The two renewable options are; our process using CO<sub>2</sub> from ethanol fermentation and wind-based electrolytic H<sub>2</sub> while the other is a process simulated in GREET based on the gasification of biomass. We chose corn as the biomass for gasification to allow for a more direct comparison between the different processes. We also compared these values to petroleum based fuels on a per energy basis. Methanol was compared to reformulated gasoline (RFG) and dimethyl ether was compared to ultra-low sulfur diesel (ULSD). Liquefied natural gas was also chosen as a comparative petroleum fuel.

Until this point we have strictly focused on CO<sub>2</sub> produced during the production of our fuels. However the biogenic CO<sub>2</sub> used in this process has not yet been accounted for. CO<sub>2</sub> emissions from fermentation processes are typically neglected as the CO<sub>2</sub> produced was originally captured by the biomass feedstock. Therefore these emissions show a net zero effect on the overall CO<sub>2</sub> emissions for the total process. For this reason we have calculated the fixed CO<sub>2</sub> in our fuels (by stoichiometric ratio) and subtracted this from the total CO<sub>2</sub> emissions (and consequently GHG emissions) for our fuels. This allows us to directly compare our emissions values to the simulated GREET fuels.

For the fuel utilization we chose to use the SIDI dedicated methanol car in GREET for the methanol fueled car. We changed the fuel in this model to be 100% methanol to allow for a direct comparison between this and our DME model. Although current technology does not utilize a 100% methanol fuel this was required for accurate data comparison. The DME car was chosen to be a CIDI vehicle running on 100% DME. Similar vehicle choices were made for the RFG, ULSD and LPG cars.

#### **5.2.2.5 Normalization to Midpoint Level**

To accurately compare impacts of different emission sources normalization is typically conducted. We chose to utilize ReCiPe 2008 as the database for characterization factors and normalization constants. Characterization factors are used to convert pollutants into a single base unit based on their individual environmental impact. This allows different pollutants to be summed into a single category based on environmental impact (i.e. global warming potential or acidification potential). Normalization then converts these totals into direct environmental impact factors that can be compared across different impact

categories. We chose to use the Midpoint Hierarchist World normalization factors found in ReCiPe and Hierarchist values for the characterization as well [115].

#### **5.2.2.6 Assumptions**

It should be noted that by changing the assumptions made in producing this life-cycle assessment, the results of this LCA can be drastically altered. A very key assumption is that economic allocation is used account for CO<sub>2</sub> emissions. Changing product costs or to exergy-based allocation would give different results. Below is a collective list of assumptions used in the collection and assembly of data for the life-cycle assessment. As well the choice of normalization factors will ultimately affect the normalized results. A different normalization method will alter results. Below is a list of assumptions made in the production of this LCA.

- Site specific turbine part production is negligible
- Decommissioning of the turbines, compressors, electrolyzers and plant equipment is beyond the scope of this work
- The integrated plant will be located in Southeast Nebraska due to the proximity to ethanol production facilities and abundance of wind energy
- Wind turbine assembly has negligible environmental effects
- Transportation of the electrolyzer and compressors is negligible
- Ethanol production is taken from GREET system
- Every gallon of ethanol produced also forms 3.08 kg CO<sub>2</sub> and 2.56 kg of DGS
- The values found in Table C.2 show allocation factors (economics based) for CO<sub>2</sub>
- Production of CO<sub>2</sub> compression and purification unit operations negligible

- Production of unit operations for the ethanol facility, CO<sub>2</sub> compression and purification and methanol/DME production are beyond the scope of this work
- Conventional and gasification based methanol and DME data were taken from the GREET platform
- Fuel use was simulated in GREET
- Midpoint Hierarchist World factors are used for characterization and normalization

## 5.3 Results and Analysis

### 5.3.1 Cradle-to-Gate Analysis

The greenhouse emissions and energy use for the methanol and dimethyl ether production can be seen in Figure 5.3 and Figure 5.4, respectively. These figures show the CO<sub>2</sub>e emissions and energy usage for the entire production process on a per metric ton product. The total value is shown divided into the burdens caused by each part of the process. A comparison between the two figures is not advised as the functional units are different.

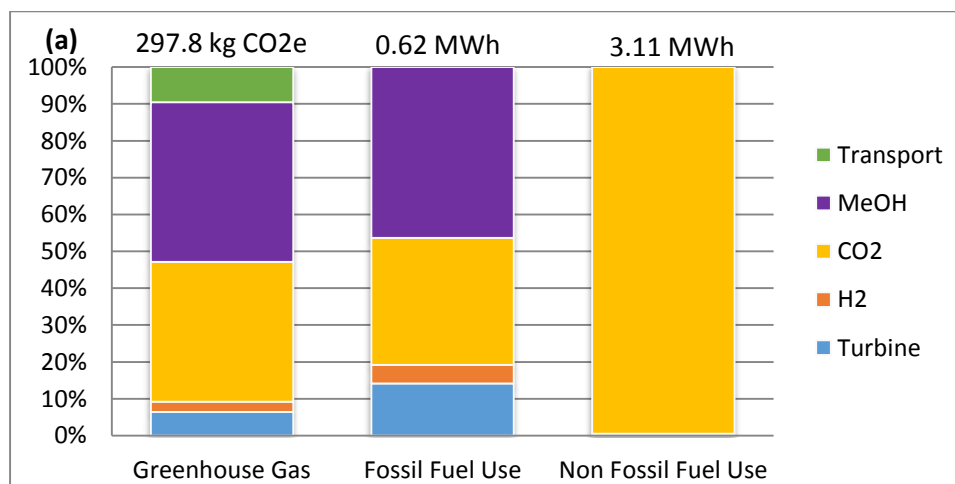


Figure 5.3: Emissions and energy use for methanol production divided by each section of the process

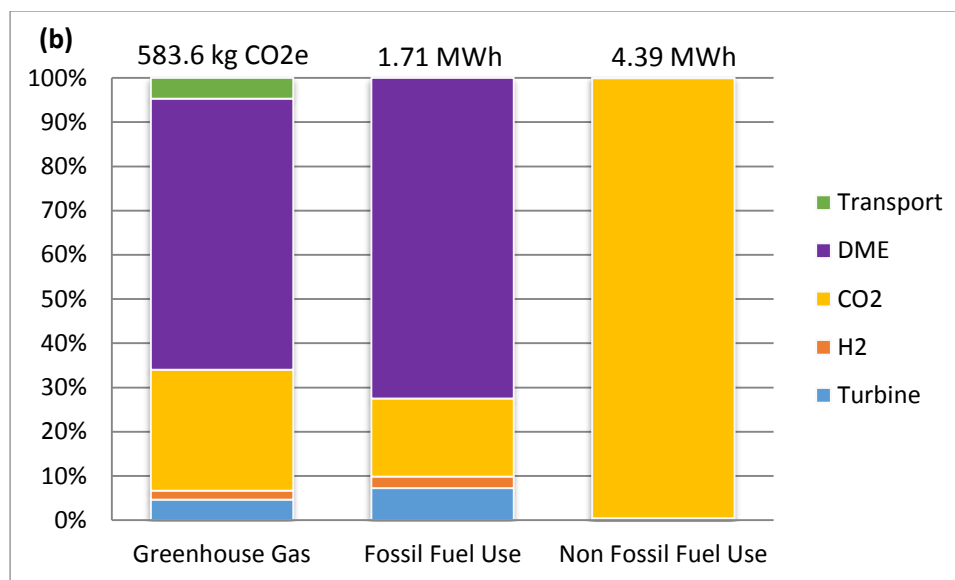


Figure 5.4: Emissions and energy use for dimethyl ether production divided by each section of the process

The clearest observation from both of these graphs is that the CO<sub>2</sub> production process uses the most non fossil fuel energy, and this should make sense as corn is the major energy input of an ethanol facility. The turbine production and electricity generation shows little impact on the data. This is likely due to the long life of the turbine and the large amount of energy it produces over this time. Although it initially has a large environmental cost this cost is largely reduced when scaled to its entire lifespan. DME production shows a larger influence on emissions and energy demand than methanol production. This is due to the higher heating requirements of the DME production, primarily coming from operating two distillation columns. The steam required for these columns is produced by natural gas combustion and produces a lot of CO<sub>2</sub>.

There exist a few metrics for comparison between different renewable and non-renewable fuels. Two primary indicators are the fossil fuel energy ratio (FER) and life cycle efficiency (LCE). The FER is defined as the ratio of the energy content of the fuel to the



fossil energy required to produce this fuel (equation 32). The LCE is the overall energy produced in methanol over the total energy consumed (shown as the ratio in equation 33).  $E_{\text{primary}}$  is any form of energy used that has not undergone any conversion processes (e.g. natural gas, wind energy, etc.).

$$\text{FER} = \frac{E_{\text{fuel}}}{E_{\text{fossil}}} \quad 32$$

$$\text{LCE} = \frac{E_{\text{fuel}}}{E_{\text{primary}} + E_{\text{fuel}}} \quad 33$$

Another environmental indicator would be the amount of  $\text{CO}_2$  that has been fixed into the chemical compared to the emissions of  $\text{CO}_2$  required to make said chemical. We have defined this metric as the carbon fixation fraction (CFF), defined in Equation 34.

$$\text{CFF} = \frac{\text{CO}_2 \text{ fixed} - \text{CO}_2 \text{e emission}}{\text{CO}_2 \text{ fixed}} \quad 34$$

The values for these metrics for both methanol and DME can be seen in .

Table 5.4.

Table 5.4: Comparative indicators for methanol and dimethyl ether facilities

	Methanol	Dimethyl Ether
FER	9.00	4.34
LCE	0.45	0.43
CFE	0.78	0.70

After normalization we were able to directly investigate a comparison of methanol and dimethyl ether production in terms of specific impact factors. We have chosen to use impact factors of human toxicity (HT), particulate matter formation (PMF), photochemical oxidant formation (POF), terrestrial acidification/acidification potential (TA) and climate change (CC) to compare our two processes. The results of this normalization can be found in Figure 5.5.

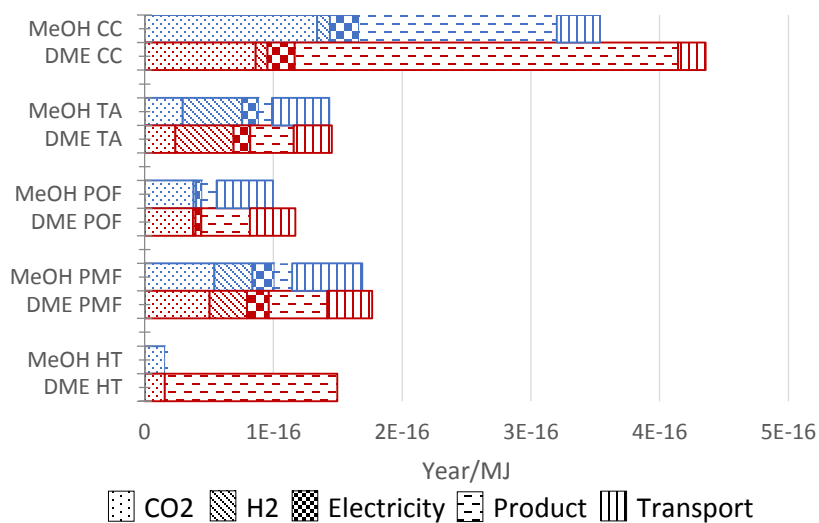


Figure 5.5: Normalized midpoint indicators for both DME (blue) and methanol (red) production processes. Impacts from individual process sections are shown as different textures

This figure was prepared using a functional unit of 1 MJ of energy, based on the lower heating value of the fuel. Both methanol (red) and dimethyl ether (blue) values are shown in the figure. As well, we have shown how the different production stages influence the

economic results (shown as different textures). This figure shows that methanol slightly outperforms dimethyl ether in most of the environmental considerations. The deciding factor for this difference is the product production stage. Again, the amount of natural gas burned for process heat in the DME process is the likely cause of this.

Non-normalized indicators for the entire processes can be found in Table 5.5. It should be noted that these values are strictly for the production stages of these chemicals (cradle-to-gate). Fuel combustion and the influence of using biogenic CO<sub>2</sub> are not accounted for.

*Table 5.5: Non-normalized environmental impacts for mt of product (methanol or dimethyl ether)*

Indicator	MeOH	DME	Unit/mt product
Global Warming Potential	0.30	0.50	mt CO <sub>2</sub> eq
Acidification Potential	0.67	0.95	kg SO <sub>2</sub> eq
Photochemical Oxidant Formation	0.69	1.13	kg NMVOC
Particulate Matter Formation	0.29	0.43	kg PM10 eq
Human Toxicity	0.10	7.68	kg 1,4-DB eq

### 5.3.2 Cradle-to-Grave Analysis

We were able to compare 3 different processes for both methanol and DME production including; our CO<sub>2</sub> hydrogenation process, a biomass gasification process, and conventional natural gas reforming process. Combustion analyses of these product fuels were compared with petroleum based fuels on a per energy basis. Methanol is compared to gasoline and dimethyl ether is compared to ultra-low sulfur diesel. Liquefied natural gas was also used as a comparison fuel as its use is becoming increasingly favored over methanol or dimethyl ether fuels. Complete tabulated results can be found in Appendix C. Figure 5.6 shows the emissions after combustion of all of these fuels. The results were compared on a per energy basis and then normalized to the largest emission value. The figure shows emissions of criteria pollutants (VOC, CO, NO<sub>x</sub> and SO<sub>x</sub>) as well as greenhouse gas emissions (GHG) and fossil fuel use (FF).

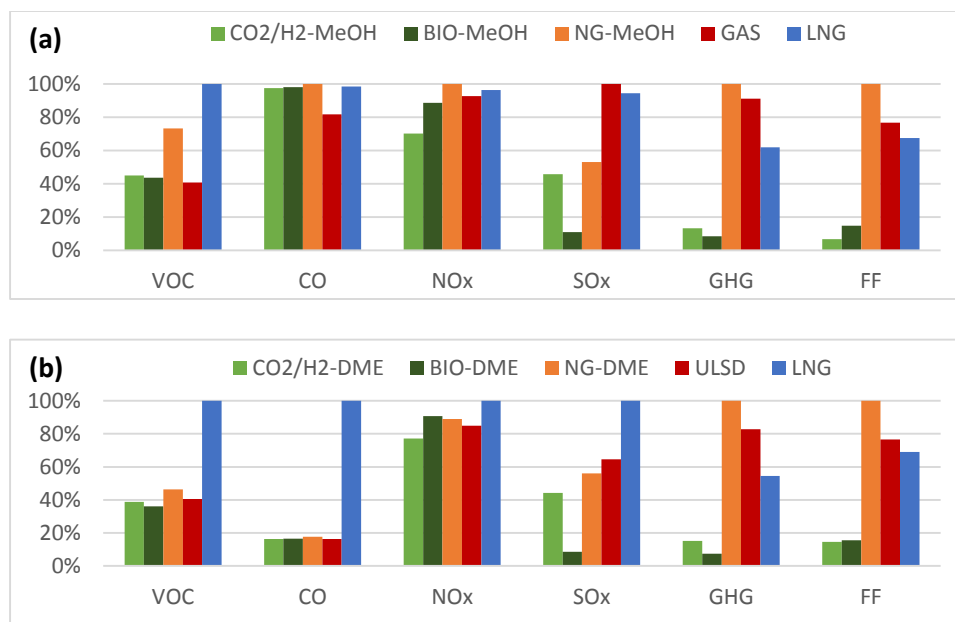


Figure 5.6: Cradle-to-grave emissions for methanol (a) and dimethyl ether (b); shown for comparison are emissions from biomass gasification based methanol and DME (BIO-MeOH/BIO-DME), natural gas based methanol and DME (NG-MeOH/NG-DME), gasoline (GAS), ultra-low sulfur diesel (ULSD) and liquefied natural gas (LNG)

Interestingly unlike the production stage DME now outperforms methanol in terms of fuel use emissions. This is due to the high emissions results for using methanol directly as a combustion fuel as well as the lower heating value that methanol has compared to dimethyl ether. The CO emissions for methanol are similar between all of the processes and this is because of the large emissions of CO during fuel use. However methanol does emit less greenhouse gasses and use less fossil fuel than DME on a per energy basis. Our process based on CO<sub>2</sub> hydrogenation is very comparable to the biomass gasification process in GREET. The major difference between the two renewable processes is SO<sub>x</sub> emissions. The majority of the SO<sub>x</sub> in the CO<sub>2</sub> hydrogenation process comes from the electrolyzer production stage. This is likely due to the processing emissions for the metals required for electrolysis. NO<sub>x</sub> emissions for the renewable processes are also high. This is because of the nitrogen fertilizer used in the farming of biomass. This fertilizer readily converts to gaseous NO<sub>x</sub> compounds and is emitted during biomass growth [107].

However, both of the renewable options largely outperform the natural gas facility and the petroleum based fuels as well. Many criteria pollutant levels would decrease by implementing these renewable fuels over petroleum based reformulated gasoline and ultra-low sulfur diesel. By implementing a CO<sub>2</sub> hydrogenation process for methanol and DME alternative fuels, greenhouse gas emissions alone can be reduced 86% and 80% over conventional petroleum based fuels, respectively. The use of our renewable methanol and DME also reduces fossil fuel depletion by 91% and 81% when compared to conventional petroleum based fuels.

#### **5.4 Conclusions**

This study demonstrates the production of renewable methanol and dimethyl ether. The use of fermentation based CO<sub>2</sub> and wind powered water electrolysis for H<sub>2</sub> production present a sustainable and environmentally friendly way to produce transportation fuels, with minimal fossil energy requirements. A life-cycle assessment shows the total environmental burdens of this production approach from well-to-wheels. ASPEN Plus was used to accurately simulate these production facilities, calculate mass and energy balances and to estimate utilities usage. GREET software was used to estimate the environmental burdens of wind turbine production, water electrolysis, ethanol fermentation for CO<sub>2</sub> production, transportation and fuel use. Environmental costs are compared between our production processes, a biomass-based gasification process, a conventional (natural gas) based process and petroleum based fuels. Emissions are compared and a normalized life-cycle impact analysis was conducted. Environmentally our renewable process is much more sustainable relying on less fossil based energy and reducing greenhouse gas emissions 82-86%, minimizing other criteria pollutants (SO<sub>x</sub>,

NO<sub>x</sub>, etc.) and reducing fossil fuel depletion by 82-91%. When determining process feasibility it is important to weigh economic and environmental factors together. While the economics behind alternative renewable fuels are still weak, peak oil and increasing petroleum prices will push the market towards more sustainable fuels. The inclusion of environmental metrics, through life-cycle assessment, in feasibility analyses is a substantial way to monitor and compare the sustainability of processes.

## **CHAPTER 6 CONCLUSIONS, RECOMMENDATIONS AND FUTURE WORK**

This work presents multiple methods of determining sustainability in quantifiable terms. Three dimensional indicators are used that balance impacts in three aspects of development; economic, environmental and societal. The indicators are defined as; material intensity, energy intensity, potential environmental impact and potential chemical risk. These indicators were applied to three different systems; chemical looping combustion, renewable methanol production and dimethyl ether production. We have applied many tools in determining metrics for these processes. Aspen Plus simulations were used to determine operating parameters like material and energy use as well as air and liquid emissions. Practical experiments were conducted for CLC to investigate the feasibility of this process. A multi-criteria decision matrix was established to apply sustainability metrics to feasibility analyses. Life-cycle assessment was also used to investigate the environmental impact a product has from cradle-to-grave. A conjunction of all these tools is necessary to accurately determine sustainability in quantifiable terms. However research is never really finished as fields are always changing and discoveries are made. With increasing environmental regulation and the demand for more environmentally conscious business planning I expect the role of sustainability assessment to increase greatly in the next 10 years, especially in the energy sector. The work conducted in CLC is far from finished. Finding the best oxygen carrier that provides high conversions and reformulations is a critical step in moving CLC forward. More research needs to be conducted in the cycling (multiple reduction/oxidation cycles) needs to be tested to understand the feasibility of a full scale plant. As well, optimized

conditions need to be discovered for these oxygen carriers. A better understanding of the kinetics and reaction mechanisms that occur in CLC would greatly aid in this. Alongside practical research into the oxygen carriers, there needs to be applied work in discovering the best methods for reaction (fixed bed, circulating fluidized bed, chemical looping oxygen uncoupling, etc.), ash removal, oxygen carrier transferring and general plant layouts that provide the highest energy efficiencies. A full life-cycle assessment of a CLC plant would also need to be conducted to see the influence that metal oxide production/disposal plays in the environmental impact of these systems.

Renewable hydrogen is also an exciting field to project into the future. While use of hydrogen directly as a fuel source may not be the best method its conversion to other fuels could be a solution to providing alternative transport fuels. The high energy density of hydrogen makes it a very versatile compound. A life-cycle assessment for various hydrogen utilization processes would be an interesting subject to investigate. As well this could be also conducted for various methanol utilization strategies as well. However, much research needs to be done in the field of electrolysis before wind-based hydrogen technologies see any economic feasibility. The low efficiencies of electrolysis make the energy efficiency of any process that utilizes such hydrogen rather low as well. These are just suggestions that future work based on these studies may develop. The tools and methods described in this work provide a broad entryway into the field of sustainability and its potential uses in the energy sector and chemical process industries.

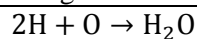


## APPENDIX A: CHEMICAL LOOPING COMBUSTION

Table A.1: Calculations completed for producing the carbon and hydrogen ratio of PRB coal used in CLC experiments

Ultimate Analysis (%)			Proximate Analysis (%)	
Carbon, wt%	Hydrogen, wt	Oxygen, wt	Moisture, wt	Ash, wt
49.65	6.72	37.70	29.39	3.45
hydrogen in moisture, wt	oxygen in moisture, wt	free hydrogen, wt	free oxygen, wt	
3.289	26.101	3.431	11.599	

Assuming Partial Free H Oxidized by Free O in Coal Through



Thus, Remaining Hydrogen and Carbon on Dry Basis for reduction of MeO Are as Follows:

$$\text{H} = 1.981\%$$

$$\text{C} = 49.65\%$$

Moles of Carbon and Hydrogen in 1 kg of Coal for Reduction of MeO

C as reducing agent, kmol	H as reducing agent, kmol
29.189	13.881

Stoichiometry Ratios

C	1
H	0.476

Table A.2: Example calculations for CuO TGA experiments for CLC

<b>Experimental Values</b>								
Initial Mass of CuO	95.974	mg						
Initial Mass of Coal	4.187	mg						
Combusted Mass Loss	13.999	mg						
Mass Gained	9.526	mg						
CO <sub>2</sub> emission	5.114	mg						
<b>Theoretical CO<sub>2</sub> Emission</b>			<b>MeO Calculations</b>			<b>Mass after Combustion</b>		
Moisture Lost	1.231	mg	CuO Required for Combustion	0.260	mmol	unreacted coal	0.146	mg
Dry Coal	2.957	mg	CuO Uncombusted	0.947	mmol	ash	0.144	mg
Mass of C	1.468	mg	Moles Cu <sub>2</sub> O Formed	0.447	mmol	formed Cu	16.524	mg
Moles of C	0.122	mmol	Moles Cu Formed	0.260	mmol	formed Cu <sub>2</sub> O	64.009	mg
Moles of CO <sub>2</sub> Produced	0.116	mmol	Moles O <sub>2</sub> Released from CuO	0.224	mmol	unreacted CuO	4.124	mg
Mass of CO <sub>2</sub> Produced	5.114	mg	Moles CuO Unreacted	0.052	mmol	Mass Remaining	84.947	mg
<b>Mass Loss Calculations</b>			<b>Reoxidation Calculations</b>			<b>% Errors</b>		
CO <sub>2</sub> Lost	5.114	mg	Moles O <sub>2</sub> captured	0.298	mmol	Mass Lost	0.000	%
Coal Moisture	1.231	mg	Moles Cu <sub>2</sub> O formed from Cu	0.130	mmol	CO <sub>2</sub> emission	0.000	%
H <sub>2</sub> O Combustion	0.498	mg	Moles O <sub>2</sub> remaining	0.233	mmol	Mass Remaining	1.411	%
O <sub>2</sub>	7.157	mg	Moles Cu <sub>2</sub> O total	0.577	mmol			
Total	13.999	mg	Moles CuO formed	0.931	mmol	Total Error	1.411	%
			Mass CuO reformed	74.041	mg			
			Total CuO	78.165	mg			
<b>% Combustion</b>	95.074	%						
<b>% Reformation</b>	81.444	%	% Conversion (CuO to Cu <sub>2</sub> O)	94.523	%			

Table A.3: Example calculations for CaSO<sub>4</sub> TGA experiments for CLC

<b>Exp. Values</b>								
Initial Mass of CaSO <sub>4</sub>	81.221	mg						
Initial mass of Coal	8.245	mg						
Combusted Mass Loss	21.640	mg						
Mass Gained	5.234	mg						
CO <sub>2</sub> emission	10.246	mg						
<b>Theoretical CO<sub>2</sub> Emission</b>			<b>MeO Calculations</b>			<b>Residual Mass</b>		
Moisture Lost	2.423	mg	Moles CaSO <sub>4</sub> Required	0.130	mmol	Ash	0.284	mg
Dry Coal	5.822	mg	Moles CaSO <sub>4</sub> Remaining	0.466	mmol	Unreacted Coal	0.008	mg
Mass of C	2.891	mg	Moles CaS Formed	0.130	mmol	Unreacted CaSO <sub>4</sub>	54.197	mg
Moles of C	0.241	mmol	CaO formed	0.091	mmol	Unreacted CaS	7.755	mg
Moles of CO <sub>2</sub> Produced	0.233	mmol	Moles CaS unreacted	0.107	mmol	Formed CaO	5.104	mg
Mass of CO <sub>2</sub> Produced	10.246	mg	Moles CaSO <sub>4</sub> unreacted	0.398	mmol	Total	67.347	mg
			Moles SO <sub>2</sub> formed	0.091	mmol			
<b>Mass Loss Calculations</b>			<b>Oxidation Calculations</b>			<b>Percent Errors</b>		
Coal Moisture	2.423	mg	Moles O <sub>2</sub> captured	0.164	mmol	Mass Loss	0.000	%
CaSO <sub>4</sub> Moisture	2.143	mg	Moles CaSO <sub>4</sub> reformed	0.082	mmol	CO <sub>2</sub> Emission	0.000	%
Combustion Moisture	0.997	mg	Mass CaSO <sub>4</sub> reformed	11.134	mg	Mass Remaining	0.705	%
CO <sub>2</sub> emission	10.246	mg	Total CaSO <sub>4</sub> remaining	65.331	mg			
SO <sub>2</sub> emission	5.831	mg				Total Error	0.705	%
Total Mass Loss	21.640	mg						
<b>% Combustion</b>	<b>96.738</b>	<b>%</b>	<b>% Conversion (CaS to CaO)</b>	<b>17.470</b>	<b>%</b>			
<b>% Reoxidation</b>	<b>80.436</b>	<b>%</b>						

Table A.4: Input and output streams for the coal CLC simulations

	COALNC	IN				OUT				
	P	WAT- IN-1	WAT- IN-2	RXNWATI N	LTAIR- IN	FLUE	ASH	WASTE <sub>H<sub>2</sub></sub> O	CO <sub>2</sub> - PROD	H <sub>2</sub> - PROD
Temp °C	25	25	25	25	25	31.1	900	102.5	21	25
P bar	1.013	1.013	1.013	1.013	1.013	1.013	22.291	1	1.013	30
Vapor Frac	0	0	0	0	1	1	0	0.32	1	1
Mass Flow kg/hr	1.25E+04	1.13E+0	1.90E+0	1.99E+04	2.16E+0	1.73E+0	4.31E+0	3.25E+04	1.59E+0	1.00E+0
Vol. Flow cum/hr		11.33	1.91	20.05	1.84E+0	1.54E+0		1.79E+04	9.71E+0	4.14E+0
Enthalpy MW	-24.72	-43.15	-7.28	-76.37	0.00	0.03	0.01	-115.82	-32.96	-0.03
Mole Frac										
OXYGEN	0	0	0	0	0.21	0.038	0	0	0	trace
CO	0	0	0	0	0	0	0	trace	0.065	0
HYDROGE N	0	0	0	0	0	0	0	1 PPB	0.071	0.999
CO <sub>2</sub>	0	0	0	0	0	0	0	4 PPM	0.839	0
WATER	0	1	1	1	0	0	0	1	0.018	0.001
H <sub>2</sub> S	0	0	0	0	0	0	0	351 PPB	0.002	0
NITROGE N	0	0	0	0	0.79	0.962	0	trace	0.006	0
METHANE	0	0	0	0	0	0	0	trace	1 PPM	0
NO <sub>2</sub>	0	0	0	0	0	3 PPM	0	0	0	0
COAL	1	0	0	0	0	0	0	0	0	0
ASH	0	0	0	0	0	0	1	0	0	0

Table A.5: Utilities for the coal CLC simulations

Utility ID:		CW	HEAT	STEAM (HPS)
Utility type:		WATER	GENERAL	STEAM
Costing rate:	\$/hr	187.37	126.02	111.99
Mass flow:	mt/hr	2.08E+03	49.42	26.04
Duty:	MW	12.07	8.24	12.44
Heating/Cooling value:	kJ/kg	-20.88	600	1.72E+03
CO <sub>2</sub> emission factor data source:			US-EPA-RULE-E9-5711	US-EPA-RULE-E9-5711
Ultimate fuel source:			NATURAL_GAS	NATURAL_GAS
CO <sub>2</sub> emission factor:	mt/GJ		5.59E-02	5.59E-02
CO <sub>2</sub> energy source efficiency factor:		1.00E+00	0.85	8.50E-01
CO <sub>2</sub> emission rate:	mt/hr		1.95	2.94
Purchase price:	\$/kg	9.00E-05	2.55E-03	4.30E-03
Electricity price:				
Inlet temperature:	C	20	1.00E+03	2.50E+02
Outlet temperature:	C	25	400	249
Inlet pressure:	bar	1.01		39.75
Outlet pressure:	bar	1.01		39.09
Inlet vapor fraction:		0		1
Outlet vapor fraction:		0		0
Inlet enthalpy:	MJ/kg	-15.89		-13.17
Outlet enthalpy:	MJ/kg	-15.87		-14.89



Table A.8: Utility usage summary for the LNG CLC simulations

Utility ID:		CW	HEAT	HIGHHEAT	HPS
Utility type:		WATER	GENERAL	GENERAL	STEAM
Costing rate:	\$/hr	3.62E+03	1.70E+03	1.88E+03	356.45
Mass flow:	mt/hr	4.02E+04	666.40	184.93	82.90
Duty:	MW	233.36	111.07	82.19	39.59
Heating/Cooling value:	kJ/kg	-20.88	600	1600	1.72E+03
CO <sub>2</sub> emission factor data source:			US-EPA-RULE-E9-5711	US-EPA-RULE-E9-5711	US-EPA-RULE-E9-5711
Ultimate fuel source:			NATURAL_GAS	NATURAL_GAS	NATURAL_GAS
CO <sub>2</sub> emission factor:	mt/GJ		5.59E-02	5.59E-02	5.59E-02
CO <sub>2</sub> energy source efficiency factor:			1	0.85	0.85
CO <sub>2</sub> emission rate:	mt/hr		26.29	19.46	9.37
Purchase price:	\$/kg	9.00E-05	2.55E-03	1.01E-02	4.30E-03
Inlet temperature:	C	20	1000	2000	250
Outlet temperature:	C	25	400	400	249
Inlet pressure:	bar	1.01			39.75
Outlet pressure:	bar	1.01			39.09
Inlet vapor fraction:		0			1
Outlet vapor fraction:		0			0
Inlet enthalpy:	MJ/kg	-15.89			-13.17
Outlet enthalpy:	MJ/kg	-15.87			-14.89

Table A.9: Overall mass and energy balances for the LNG CLC simulation

COMPONENTS (KMOL/HR)	IN	OUT
WATER	4.14E+03	3.50E+03
METHANE	950	7.76E-05
HYDROGEN	0	2.64E+03
OXYGEN	1.79E+03	1.09E+03
NITROGEN	6.74E+03	6.74E+03
ETHANE	20	0
PROPANE	10	0
CO <sub>2</sub>	0	1020
TOTAL BALANCE		
MASS(KG/HR)	3.37E+05	3.37E+05
ENTHALPY(MW)	-299.82	-140.81

## APPENDIX B: METHANOL PRODUCTION

*Table B.1: Estimated U.S. average levelized cost of electricity (LCE) with 2012 \$/MWh for renewable advanced generation resources entering service in 2019*

Plant type	Capacity factor (%)	LCE	O & M with fuel	Transmission investment	Total LCE
Geothermal	92	34.2		1.4	47.9
Biomass	83	47.4	39.5	1.2	102.6
Wind	35	64.1		3.2	80.3
Wind-Offshore	37	175.4		5.8	204.1
Solar PV	25	114.5		4.1	130.0
Solar thermal	20	195.0		6.0	243.1
Hydro	53	72.0	6.0	2.0	84.5

O & M: Operations and Maintenance cost; PV: Photovoltaic

Table B.2: Stream tables highlighting the input and output streams for the methanol production facility

	H2-IN	CO <sub>2</sub> -IN	METHANOL	WWATER	NET-FLUE	BFW	STEAM
Temperature °C	25	-25.6	25	25	24.9	233	233
Pressure bar	33	16.422	1.013	1.013	1.013	30	30
Vapor Frac	1	0	0	0	1	0	1
Mole Flow kmol/hr	383.676	131	126.421	126.106	9.077	214.575	214.575
Mass Flow mt/day	18.5637	138.367	97.011	54.643	5.284	92.775	92.775
Volume Flow cum/hr	293.911	5.473	5.093	2.294	221.683	5.097	266.687
Enthalpy Gcal/hr	0.003	-12.817	-7.333	-8.702	-0.44	-13.84	-12.103
Mass Fraction							
CO <sub>2</sub>		1	0.002	trace	0.86		
CO					trace		
H <sub>2</sub>	1		trace		0.037		
H <sub>2</sub> O			0.003	0.995	0.004	1	1
Methanol			0.995	0.005	0.098		
Mole Fraction							
CO <sub>2</sub>		1	0.001	trace	0.474		
CO					trace		
H <sub>2</sub>	1		6 PPB		0.446		
H <sub>2</sub> O			0.006	0.997	0.006	1	1
Methanol			0.993	0.003	0.074		



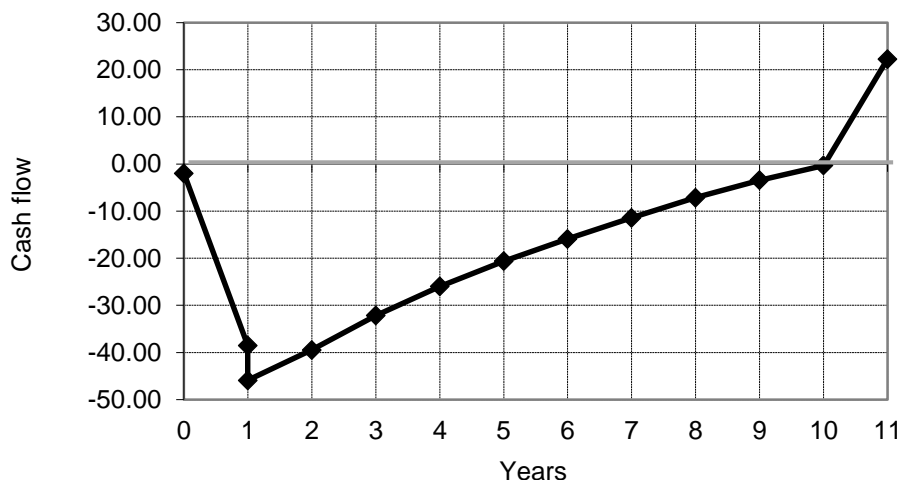


Figure B.1: Plot of the discounted cash flow of the integral methanol plant over 10 years of operation with H<sub>2</sub> selling price = \$0.30/kg H<sub>2</sub>; methanol selling price \$485/mt methanol. \*CDCF: Cumulative Discounted Cash Flow; FCI: Fixed capital investment = \$38.5 M; WC: Working capital = \$7.7 M; D: Depreciation (Maximum accelerated Cost Recovery System); R: Revenue = \$20.04 M; COP: Cost of production = \$13.99 M; L: Cost of land = \$2 M; S: Salvage value = \$9.85 M; NPV: Net present value; t: tax = 35%, and i: interest rate of bank loan = 5.25%

Table B.3: Calculated values of the economic decision factors from the above DCFD

EC	0.635
PC, \$/mt	406.32
NPV, M\$	22.22
ROR, %	26.95
PBP, years	7.52

### Cost Calculations

$$\text{Cost of Production} = 0.18\text{FCI} + 2.73(\text{COL}) + 1.23(\text{CRM} + \text{CWM} + \text{CUT}) \quad \text{B1}$$

$$\text{Revenue} = (\text{MeOH}_{\text{price}}\text{MeOH}_{\text{flow}} + \text{O}_2_{\text{price}}\text{O}_2_{\text{flow}} + \text{CO}_2_{\text{credit}}) \times \text{OH} \quad \text{B2}$$

$$\text{Plant Capacity} = \text{OH} \times \text{Hourly production of methanol} \quad \text{B3}$$

where: COL = Cost of Labor; CRM = Cost of Raw Materials; CWM = Cost of Waste

Management; CUT = Cost of Utilities; OH = Operational hours per year

## APPENDIX C: LIFE-CYCLE ASSESSMENT

*Table C.1: Transportation data collected and used for the transport of individual turbine components*

<b>Component</b>	<b>mass (ton)</b>	<b>location</b>	<b>distance (km)</b>	<b>mass-distance (tkm)</b>
Blades	20.07	Windsor, CO	761.5	1.528E+04
Rotor	19.93	Brighton, CO	753.0	1.501E+04
Gearbox	24.06	Lake Zurich, IL	848.6	2.042E+04
Generator	7.14	Raleigh, NC	2037.9	1.455E+04
Yaw/Pitch system	11.82	Hebron, KY	1246.1	1.473E+04
Tower	160	Pueblo, CO	969.6	1.551E+05
Nacelle	24.98	Brighton, CO	753.0	1.881E+04

*Table C.2: Calculation of allocation factors for the ethanol production facility*

<b>Compound</b>	<b>Flow</b>	<b>Cost</b>	<b>Cost Flow (\$/mt CO<sub>2</sub>)</b>	<b>Allocation factor (%)</b>
CO <sub>2</sub>	3.08 kg	\$40/mt	40	6.1
Ethanol	1 gallon	\$1.43/gal	463.45	71.0
DGS	2.56 kg	\$180/mt	149.16	22.9

Table C.3: Total cradle-to-gate emissions and energy use for producing a metric ton of CO<sub>2</sub>, H<sub>2</sub>, methanol and dimethyl ether.

	CO <sub>2</sub>	H <sub>2</sub>	MeOH	DME	Unit per mt product
<b>Criteria Pollutants</b>					
VOC	43.7	25.0	90.0	202.4	g
CO	43.0	227.7	208.6	419.4	g
NO <sub>x</sub>	138.0	197.3	589.8	936.8	g
PM <sub>10</sub>	22.6	72.4	61.0	90.7	g
PM <sub>2.5</sub>	7.9	35.8	32.0	49.5	g
SO <sub>x</sub>	18.9	1321.5	338.8	450.3	g
CH <sub>4</sub>	4.9	224.8	229.9	940.5	g
N <sub>2</sub> O	96.4	1.3	283.5	401.9	g
CO <sub>2</sub>	51.4	134.8	-1240.1	-1499.9	kg
SF <sub>6</sub>	0.0	4.4	2.0	2.9	mg
C <sub>2</sub> F <sub>6</sub>	0.0	0.5	0.1	0.1	mg
Black carbon	1.4	1.2	2.9	6.1	g
POC	1.3	2.1	5.2	12.2	g
<b>Greenhouse Gas</b>	78.4	142.5	-1128.5	-1412.7	kg
<b>Energy Use</b>					
Fossil Fuel	148.4	615.3	619.5	1829.5	kWh
Coal Fuel	10.5	246.1	63.9	93.0	kWh
Natural Gas Fuel	134.2	296.8	535.1	1704.3	kWh
Petroleum Fuel	3.7	72.4	20.5	32.3	kWh
Non Fossil Fuel	2149.3	63.3	3103.8	4348.0	kWh
Nuclear	0.1	36.8	7.5	11.0	kWh
Renewable	2149.2	26.5	3096.3	4336.9	kWh

## **PUBLICATIONS LIST (RELEVANT TO THESIS)**

- 1) "CaSO<sub>4</sub>-based chemical-looping combustion of coal with CO<sub>2</sub> capture," EPRI, Palo Alto, CA, 2015.
- 2) Y. Demirel, M. Matzen, C. Winters and X. Gao, "Capturing and Using CO<sub>2</sub> as Feedstock with Chemical Looping and Hydrothermal Technologies," *International Journal of Energy Research*, vol. 39, pp. 1011-1047, 2015.
- 3) M. Matzen, M. Alhajji and Y. Demirel, "Chemical storage of wind energy by renewable methanol production: Feasibility analysis using a multi-criteria decision matrix," *Energy*, vol. 93, pp. 343-353, 2015.
- 4) M. Matzen, M. Alhajji and Y. Demirel, "Technoeconomics and sustainability of renewable methanol and ammonia productions using wind power-based hydrogen," *Advanced Chemical Engineering*, vol. 5, no. 3, p. 128, 2015.
- 5) M. Matzen and Y. Demirel, "Methanol and dimethyl ether from renewable hydrogen and carbon dioxide: Alternative fuels production and life-cycle assessment", submitted to *Chemical Engineering Journal*

## REFERENCES

- [1] A. A. Martins, T. M. Mata, C. A. Costa and S. K. Sikdar, "Framework for sustainability metrics," *Industrial Engineering and Chemistry Resource*, vol. 46, pp. 2962-2973, 2007.
- [2] H. der Bruijn, R. van Duin and M. A. Huijbregts, *Handbook on life cycle assessment*, New York: Kluwer Academic Publishers, 2004.
- [3] ISO/IEC, "ISO 14040:2006 Environmental management -- Life cycle assessment -- Principles and framework," ISO/IEC, 2006.
- [4] ISO/IEC, "ISO 14044:2006 Environmental management -- Life cycle assessment -- Requirements and guidelines," ISO/IEC, 2006.
- [5] Scientific Applications International Corporation, "Life cycle assessment: Principles and Practice," EPA, 2006.
- [6] N. von der Assen, P. Voll, M. Peters and A. Bardow, "Life cycle assessment of CO<sub>2</sub> capture and utilization: a tutorial review," *Chem. Soc. Rev.*, vol. 43, pp. 7982-7994, 2014.
- [7] J. Owens, "Life-Cycle Assessment: Constraints on moving from inventory to impact assessment," *Journal of Industrial Ecology*, vol. 1, no. 1, pp. 37-49, 1997.
- [8] "CaSO<sub>4</sub>-based chemical-looping combustion of coal with CO<sub>2</sub> capture," EPRI, Palo Alto, CA, 2015.
- [9] Y. Demirel, M. Matzen, C. Winters and X. Gao, "Capturing and Using CO<sub>2</sub> as Feedstock with Chemical Looping and Hydrothermal Technologies," *International Journal of Energy Research*, vol. 39, pp. 1011-1047, 2015.

- [10] M. Matzen, M. Alhajji and Y. Demirel, "Chemical storage of wind energy by renewable methanol production: Feasibility analysis using a multi-criteria decision matrix," *Energy*, vol. 93, pp. 343-353, 2015.
- [11] J. M. Melilo, R. Terece (T.C.) and G. W. Yohe, "Climate change impacts in the United States: The third national climate assessment," U.S. Global Change Research Program, 2014.
- [12] EPA, "Future Climate Change," EPA, 21 July 2015. [Online]. Available: <http://www.epa.gov/climatechange/science/future.html>. [Accessed 2 September 2015].
- [13] B. R. Singh and O. Singh, "Global trends of fossil fuel reserves and climate change in the 21st century," in *Fossil fuel and the environment*, InTech, 2012, pp. 167-192.
- [14] S. Saeidi, N. A. S. Amin and M. R. Rahimpour, "Hydrogenation of CO<sub>2</sub> to value-added production-A review and potential future developments," *Journal of CO<sub>2</sub> utilization*, vol. 5, pp. 66-81, 2014.
- [15] G. Aydin, I. Karakurt and K. Aydiner, "Evaluation of geologic storage options of CO<sub>2</sub>: Applicability, cost, storage capacity and safety," *Energy Policy*, vol. 38, no. 9, pp. 5072-5080, 2010.
- [16] Y. Cao and W.-P. Pan, "Investigation of chemical looping combustion by solid fuels: Process analysis," *Energy and Fuels*, vol. 20, pp. 1836-1844, 2006.
- [17] R. Siriwardane, H. Tian, G. Richards, T. Simonyi and J. Poston, "Chemical-looping combustion of coal with metal oxide oxygen carriers," *Energy and Fuels*, vol. 23, pp. 3885-3892, 2009.

- [18] Q. Guo, J. Zhang and H. Tian, "Recent advances in CaSO<sub>4</sub> oxygen carrier for chemical-looping combustion (clc) process," *Chemical Engineering Communications*, vol. 199, pp. 1463-1491, 2012.
- [19] T. Proll, K. Mayer, J. Bolhar-Nordenkamp, P. Kolbitsch, T. Mattisson, A. Lyngfelt and H. Hofbauer, "Natural minerals as oxygen carriers for chemical looping combustion in a dual circulating fluidized bed system," *Energy Procedia*, vol. 1, pp. 27-34, 2009.
- [20] Y. Zhu, K. Mimura, J.-W. Lim, M. Isshiki and Q. Jiang, "Brief review of oxidation kinetics of copper at 350C to 1050C," *Metallurgical and Materials Transactions A*, vol. 37A, pp. 1231-1237, 2006.
- [21] G. Marban, M. Garcia-Calzada and A. Fuertes, "Kinetics of oxidation of CaS particles in the regime of low SO<sub>2</sub> release," *Chemical Engineering Science*, vol. 54, pp. 77-90, 1998.
- [22] Aspen Technology, Inc., *Aspen Plus*, Burlington, MA, 2014.
- [23] Y. Demirel, *Energy; Production, Conversion, Storage, Conservation, and Coupling*, London: Springer, 2012.
- [24] U.S. Energy Information Administration, "Annual Energy Outlook," 2014.
- [25] E. Lantz, M. Hand and R. Wiser, "2010 Wind Technologies Market Report," 2011.
- [26] P. Esmaili, I. Dincer and G. Naterer, "Energy and Exergy Analyses of Electrolytic Hydrogen Production with Molybdenum-Oxo Catalysts," *International Journal of Hydrogen Energy*, vol. 37, no. 9, pp. 7365-7372, May 2012.

- [27] A. Tremel, P. Wasserscheid, M. Baldauf and T. Hammer, "Techno-economic analysis for the synthesis of liquid and gaseous fuels based on hydrogen production via electrolysis," *International Journal of Hydrogen Energy*, vol. 40, no. 35, pp. 11457-11464, 2015.
- [28] I. Dincer and C. Acar, "Review and evaluation of hydrogen production methods for better sustainability," *International Journal of Hydrogen Energy*, vol. 40, pp. 11094-11111, 2015.
- [29] A. Dingizian, J. Hansson, T. Persson, H. Svensson Ekberg and P. Tuna, "A Feasibility Study on Integrated Hydrogen Production," 2007. [Online]. Available: <http://www.chemeng.lth.se/ket050/Finalreport/HydroHydrogen.pdf>. [Accessed 10 August 2014].
- [30] "Norsk Electrolyzer," [Online]. Available: [http://large.stanford.edu/courses/2010/ph240/pushkarev2/docs/norsk\\_electrolysers.pdf](http://large.stanford.edu/courses/2010/ph240/pushkarev2/docs/norsk_electrolysers.pdf). [Accessed 10 August 2014].
- [31] B. D. James, J. M. Moton and W. G. Colella, "Guidance for Filling Out a Detailed H<sub>2</sub>A Production Case Study [Presentation Slides]," 2013. [Online]. Available: [http://energy.gov/sites/prod/files/2014/03/f12/webinar\\_slides\\_h2a\\_production\\_analysis\\_070913.pdf](http://energy.gov/sites/prod/files/2014/03/f12/webinar_slides_h2a_production_analysis_070913.pdf). [Accessed 10 August 2014].
- [32] P. G. Jessop, F. Joo and C.-C. Tai, "Recent advances in the homogeneous hydrogenation of carbon dioxide," *Coordination Chemistry Reviews*, vol. 248, no. 21-24, pp. 2425-2442, 2004.



- [33] S. Moret, P. J. Dyson and G. Laurency, "Direct synthesis of formic acid from carbon dioxide by hydrogenation in acidic media," *Nature Communications*, vol. 5, pp. 1-7, 2014.
- [34] C. Wu, Z. Zhang, Q. Zhu, H. Han, Y. Yingying and B. Han, "Highly efficient hydrogenation of carbon dioxide to methyl formate over supported gold catalysts," *Green Chemistry*, vol. 17, pp. 1467-1472, 2015.
- [35] M. K. Gnanamani, G. Jacobs, R. A. Keogh, W. D. Shafer, D. E. Sparks, S. D. Hopps, G. A. Thomas and B. H. Davis, "Fischer-Tropsch synthesis: Effect of pretreatment conditions of cobalt on activity and selectivity for hydrogenation of carbon dioxide," *Applied Catalysis A: General*, vol. 499, pp. 39-46, 2015.
- [36] S. G. Jadhav, P. D. Vaidya, B. M. Bhanage and J. B. Joshi, "Catalytic carbon dioxide hydrogenation to methanol: A review of recent studies," *Chemical Engineering Research and Design*, vol. 92, no. 11, pp. 2557-2567, 2014.
- [37] Methanol Institute, "The Methanol Industry," Methanol Institute, 2011. [Online]. Available: <http://www.methanol.org/Methanol-Basics/The-Methanol-Industry.aspx>. [Accessed 2015 2 September].
- [38] New World Encyclopedia, "Methanol," 21 October 2014. [Online]. Available: <http://www.newworldencyclopedia.org/p/index.php?title=Methanol&oldid=984943>. [Accessed 28 August 2015].
- [39] M. Manning, "Driven by China, global methanol demand rises 23 percent in two years, unprecedented demand growth expected for 2012 to 2022, says new IHS study," IHS, 11 March 2013. [Online]. Available: <http://press.ihs.com/press->

release/country-industry-forecasting/driven-china-global-methanol-demand-rises-23-percent-two-. [Accessed 31 August 2015].

- [40] J. Chesko, "Methanol industry outlook [Presentation Slides]," Methanex, May 2014.
- [41] S. Shafiee and E. Topal, "When will fossil fuel reserves be diminished?," *Energy Policy*, vol. 37, no. 1, pp. 181-189, 2009.
- [42] Methanex, "Methanex monthly average regional posted contract price history," 31 August 2015. [Online]. Available: [https://www.methanex.com/sites/default/files/methanol-price/MxAvgPrice\\_Aug%2031%202015.pdf](https://www.methanex.com/sites/default/files/methanol-price/MxAvgPrice_Aug%2031%202015.pdf). [Accessed 31 August 2015].
- [43] U.S. Energy Information Administration, "Petroleum & other liquids; Spot Prices," October 2015.
- [44] G. A. Olah, "Beyond oil and gas: The methanol economy," *Angewandte Chemie International Edition*, vol. 44, no. 18, pp. 2636-2639, 2005.
- [45] G. A. Olah, A. Goeppert and G. S. Prakash, "Chemical recycling of carbon dioxide to methanol and dimethyl ether: From greenhouse gas to renewable, environmentally carbon neutral fuels and synthetic hydrocarbons," *Journal of Organic Chemistry*, vol. 74, no. 2, pp. 487-498, 2009.
- [46] MMSA, "MMSA methanol supply and demand balance," Methanol Market Services Asia, 2013.
- [47] L. K. Rihko-Struckmann, A. Peschel, R. Hanke-Rauschenbach and K. Sundmacher, "Assessment of Methanol Synthesis Utilizing Exhaust CO<sub>2</sub> for

- Chemical Storage of Electrical Energy," *Industrial and Engineering Chemistry Research*, vol. 49, no. 21, pp. 11073-11078, 2010.
- [48] E. S. Van-Dal and C. Bouallou, "CO<sub>2</sub> abatement through a methanol production process," *Chemical Engineering Transactions*, vol. 29, pp. 463-468, 2012.
- [49] E. S. Van-Dal and C. Bouallu, "Design and simulation of a methanol production plant from CO<sub>2</sub> hydrogenation," *Journal of Cleaner Production*, vol. 57, pp. 38-45, 2013.
- [50] F. Pontzen, W. Liebner, V. Gronemann, M. Rothaemel and B. Ahlers, "CO<sub>2</sub>-based methanol and DME - Efficient technologies for industrial scale production," *Catalysis Today*, vol. 171, no. 1, pp. 242 - 250, 2011.
- [51] D. Mignard, M. Sahibzada, J. M. Duthie and H. W. Whittington, "Methanol synthesis from flue-gas CO<sub>2</sub> and renewable electricity: A feasibility study," *International Journal of Hydrogen Energy*, vol. 28, no. 4, pp. 455-464, 2003.
- [52] P. J. Woolcock and R. C. Brown, "A review of cleaning technologies for biomass-derived syngas," *Biomass and Bioenergy*, vol. 52, pp. 54-84, 2013.
- [53] K. A. Ali, A. Z. Abdullah and A. R. Mohamed, "Recent development in catalytic technologies for methanol synthesis from renewable sources: A critical review," *Renewable and Sustainable Energy Reviews*, vol. 44, pp. 508-518, 2015.
- [54] A. Theophilus, "Control structure design for methanol process (Master's thesis)," NTNU-Trondheim, 2010.
- [55] L. Chen, Q. Jiang, Z. Song and D. Posarac, "Optimization of Methanol Yield from a Lurgi Reactor," *Chemical Engineering and Technology*, vol. 34, no. 5, pp. 817-822, 2011.

- [56] J. A. Moulijn, M. Makkee and A. E. Van Diepen, "Methanol," in *Chemical Process Technology*, Chichester, West Sussex, United Kingdom, Wiley, 2013, pp. 191-201.
- [57] K. M. Holmgren, T. Berntsson, E. Andersson and T. Rydberg, "System aspects of biomass gasification with methanol synthesis - Process concepts and energy analysis," *Energy*, vol. 45, pp. 817-828, 2012.
- [58] D. Baruah and D. Baruah, "Modeling of biomass gasification: A review," *Renewable and Sustainable Energy Reviews*, vol. 39, pp. 806-815, 2014.
- [59] N. Shamsul, S. Kamarudin, N. Rahman and N. Kofli, "An overview on the production of bio-methanol as potential renewable energy," *Renewable and Sustainable Energy Reviews*, vol. 33, pp. 578-588, 2014.
- [60] C. J. Koroneos, A. T. Dompros, G. Roumbas and N. Moussiopoulos, "Life cycle assessment of hydrogen fuel production processes," *International Journal of Hydrogen Energy*, vol. 29, pp. 1443-1450, 2004.
- [61] R. Bhandari, C. A. Trudewind and P. Zapp, "Life cycle assessment of hydrogen production via electrolysis - a review," *Journal of Cleaner Production*, vol. 85, pp. 151-163, 2014.
- [62] NEL Hydrogen, "Efficient electrolyzers for hydrogen production," [Online]. Available: [http://wpstatic.idium.no/www.nel-hydrogen.com/2015/03/Efficient\\_Electrolysers\\_for\\_Hydrogen\\_Production.pdf](http://wpstatic.idium.no/www.nel-hydrogen.com/2015/03/Efficient_Electrolysers_for_Hydrogen_Production.pdf). [Accessed 26 September 2015].
- [63] I. Dincer, "Green methods for hydrogen production," *International Journal of Hydrogen Energy*, vol. 37, pp. 1954-1971, 2012.

- [64] NEL Hydrogen, "50 MW H<sub>2</sub> Plant," [Online]. Available:  
[http://wpstatic.idium.no/www.nel-hydrogen.com/2015/04/NEL\\_Hydrogen\\_50MW.pdf](http://wpstatic.idium.no/www.nel-hydrogen.com/2015/04/NEL_Hydrogen_50MW.pdf). [Accessed 26 September 2015].
- [65] M. Maack, "Generation, of the energy carrier hydrogen," NEEDS, 2008.
- [66] T. Grant, "Carbon Dioxide Transport and Storage Costs in NETL Studies," National Energy Technology Laboratory, 2013.
- [67] R. Finely, "Evaluation of CO<sub>2</sub> capture options from ethanol plants," 2006. [Online]. Available:  
[http://sequestration.org/resources/publish/phase2\\_capture\\_topical\\_rpt.pdf](http://sequestration.org/resources/publish/phase2_capture_topical_rpt.pdf).
- [68] International Energy Agency, "Technology Roadmap: Energy and GHG Reductions in the Chemical Industry via Catalytic Processes," 2013.
- [69] J. Toyir, R. Miloua, N. Elkadri, M. Nawdali, H. Toufik, F. Miloua and M. Saito, "Sustainable Process for the Production of Methanol from CO<sub>2</sub> and H<sub>2</sub> Using Cu/ZnO-Based Multicomponent Catalyst," *Physics Procedia*, vol. 2, no. 3, pp. 1075-1079, 2009.
- [70] C. P. Galindo and O. Badr, "Renewable Hydrogen Utilisation for the Production of Methanol," *Energy Conversion and Management*, vol. 48, no. 2, pp. 519-527, February 2007.
- [71] S. Weiduan, J. Zhang, Z. Bingchen, W. Hongshi, F. Dingye, Z. Mingjia and S. Qiwen, "Kinetics of Methanol Synthesis in the Presence of C301 Cu-Based Catalyst (I) Intrinsic and Global Kinetics," *Journal of Chemical Industry and Engineering (China)*, vol. 4, no. 2, pp. 248-257, 1989.

- [72] L. Chen, Q. Jiang, Z. Song and D. Posarac, "Optimization of methanol yield from a Lurgi reactor," *Chemical Engineering Technology*, vol. 34, pp. 817-822, 2011.
- [73] B. Anicic, P. Trop and D. Goricanec, "Comparison between two methods of methanol production from carbon dioxide," *Energy*, vol. 77, pp. 279-289, 2014.
- [74] "Economic Indicators," *Chemical Engineering Essentials for the CPI Professional*, p. 72, February 2015.
- [75] R. Turton, R. C. Bailie, W. B. Whiting, J. A. Shaeiwitz and D. Bhattacharyya, *Analysis, Synthesis and Design of Chemical Processes*, 4 ed., Upper Saddle River: Prentice Hall, 2012.
- [76] G. Saur, "Wind-to-Hydrogen Project: Electrolyzer Capital Cost Study," National Renewable Energy Laboratory, Golden, CO, 2008.
- [77] G. Saur, C. Ainscough, K. Harrison and T. Ramsden, "Hour-by-Hour Cost Modeling of Optimized Central Wind-Based Water Electrolysis Production [Presentation Slides]," National Renewable Energy Laboratory, Golden, CO, 2013.
- [78] International Energy Agency, "Hydrogen production and storage: R&D priorities and gaps," 2006.
- [79] H. T. Luk, H. M. Lei, W. Y. Ng, Y. Ju and K. F. Lam, "Techno-Economic Analysis of Distributed Hydrogen Production from Natural Gas," *Chinese Journal of Chemical Engineering*, vol. 20, no. 3, pp. 489-496, 2012.
- [80] S. Faberi, L. Paolucci, D. Velte and I. Jimenex, "Methanol: a Future Transport Fuel Based on Hydrogen and Carbon Dioxide? Economic Viability and Policy Options," *Science and Technology Options Assessment*, Brussels, 2014.

- [81] Z. Jiang, T. Xiao, V. L. Kuznetsov and P. P. Edwards, "Turning Carbon Dioxide into Fuel," *Philosophical Transactions of the Royal Society A*, vol. 368, pp. 3343-3364, 2010.
- [82] G. A. Olah, A. Goeppert and G. K. Surya Prakash, *Beyond Oil and Gas: The Methanol Economy*, 2 ed., New York: Wiley, 2011.
- [83] Y. Demirel, "Sustainable Operations for Distillation Columns," *Chemical Engineering and Process Techniques*, vol. 1005, pp. 1-15, 2013.
- [84] K. Kowalski, S. Stagl, R. Madlener and I. Omann, "Sustainable energy futures: Methodological challenges in combining scenarios and participatory multi-criteria analysis," *European Journal of Operational Research*, vol. 197, no. 3, pp. 1069-1074, 2009.
- [85] S. Pugh, "Concept Selection: a Method that Works," in *Proceedings International Conference on Engineering Design*, Zurich, 1981.
- [86] M. Matzen, M. Alhajji and Y. Demirel, "Technoeconomics and sustainability of renewable methanol and ammonia productions using wind power-based hydrogen," *Advanced Chemical Engineering*, vol. 5, no. 3, p. 128, 2015.
- [87] T. A. Semelsberger, R. L. Borup and H. L. Greene, "Dimethyl ether (DME) as an alternative fuel," *Journal of Power Sources*, vol. 156, pp. 497-511, 2006.
- [88] Y. Zhu, S. Tjokro Rahardjo, C. Valkenburg, L. Snowden-Swan, S. Jones and M. Machinal, "Techno-economic analysis for the thermochemical conversion of biomass to liquid fuels," U.S. Department of Energy, 2011.

- [89] N. Khandan, M. Kazemeini and M. Aghaziarati, "Direct production of dimethyl ether from synthesis gas utilizing bifunctional catalysts," *Applied Petrochemical Research*, vol. 1, no. 1, pp. 21-27, 2012.
- [90] M. Mollavali, F. Yaripour, H. Atashi and S. Sahebdehfar, "Intrinsic kinetics study of dimethyl ether synthesis from methanol on gamma-Al<sub>2</sub>O<sub>3</sub> catalysts," *Industrial and Engineering Chemistry Research*, vol. 47, pp. 3265-3273, 2008.
- [91] A. Quek and R. Balasubramanian, "Life cycle assessment of energy and energy carriers from waste matter - A review," *Journal of Cleaner Production*, vol. 79, pp. 18-31, 2014.
- [92] M. L. G. Reno, E. E. S. Lora, J. C. E. Palacio, O. J. Venturini, J. Buchgeister and O. Almazan, "A LCA (life cycle assessment) of the methanol production from sugarcane bagasse," *Energy*, vol. 36, pp. 3716-3726, 2011.
- [93] M. L. G. Reno, E. E. S. Lora, O. J. Venturini and J. C. E. Palacio, "Life cycle assessment of the methanol production from sugarcane bagasse considering two different alternatives of energy supply," in *20th International Congress of Mechanical Engineering*, Gramado, RS, Brazil, 2009.
- [94] K. M. Holmgren, E. Andersson, T. Berntsson and T. Rydberg, "Gasification-based methanol production from biomass in industrial clusters: Characterization of energy balances and greenhouse gas emissions," *Energy*, vol. 69, pp. 622-637, 2014.
- [95] M. Wu, Y. Wu and M. Wang, "Energy and emission benefits of alternative transportation liquid fuels derived from switchgrass: A fuel life cycle assessment," *Biotechnology Progress*, vol. 22, pp. 1012-1024, 2006.



- [96] The University of California, Davis; The University of California, Berkeley, "California Dimethyl Ether Multimedia Evaluation," California Environmental Protection Agency Multimedia Working Group, 2014.
- [97] M. Higo and K. Dowaki, "A life cycle analysis on a bio-DME production system considering the species of biomass feedstock in Japan and Papua New Guinea," *Applied Energy*, vol. 87, no. 1, pp. 58-67, 2009.
- [98] K. C. Tokay, T. Dogu and G. Docu, "Dimethyl ether synthesis over alumina based catalysts," *Chemical Engineering Journal*, vol. 184, pp. 278-285, 2012.
- [99] M. Farsi, R. Eslamloueyan and A. Jahanmiri, "Modeling, simulation and control of dimethyl ether synthesis in an industrial fixed-bed reactor," *Chemical Engineering and Processing: Process Intensification*, vol. 50, pp. 85-94, 2011.
- [100] M. Fazlollahnejad, M. Taghizadeh, A. Eliassi and G. Bakeri, "Experimental study and modeling of an adiabatic fixed-bed reactor for methanol dehydration to dimethyl ether," *Chinese Journal of Chemical Engineering*, vol. 17, no. 4, pp. 630-634, 2009.
- [101] P. L. Spath and M. K. Mann, "Life cycle assessment of renewable hydrogen production via wind/electrolysis," National Renewable Energy Laboratory, Golden, CO, 2004.
- [102] R. H. Crawford, "Life cycle energy and greenhouse emissions analysis of wind turbines and the effect of size on energy yield," *Renewable and Sustainable Energy Reviews*, vol. 13, pp. 2653-2660, 2009.

- [103] E. Martinez, F. Sanz, S. Pllegirini, E. Jimenez and J. Blanco, "Life cycle assessment of a multi-megawatt wind turbine," *Renewable Energy*, vol. 34, pp. 667-673, 2009.
- [104] K. R. Haapala and P. Prempreeda, "Comparative life cycle assessment of 2.0 MW wind turbines," *International Journal of Sustainable Manufacturing*, vol. 3, no. 2, pp. 170-185, 2014.
- [105] M. Wang, H. Huo and S. Arora, "Methods of dealing with co-products of biofuels in life-cycle analysis and consequent results within the U.S. context," *Energy Policy*, vol. 39, pp. 5726-5736, 2011.
- [106] M. Wang, M. Wu and H. Huo, "Life-cycle energy and greenhouse gas emission impacts of different corn ethanol plant types," *Environmental Research Letters*, vol. 2, pp. 1-13, 2007.
- [107] Z. Wang, J. B. Dunn and M. Q. Wang, "Updates to the corn ethanol pathway and development of an integrated corn and corn stover ethanol pathway in the GREET model," Argonne National Laboratory - Energy Systems Division, 2014.
- [108] D. Lorenz and D. Morris, "How much energy does it take to make a gallon of ethanol?," Institute for Local Self-Reliance, Minneapolis, MN, 1995.
- [109] N. von der Assen, J. Jung and A. Bardow, "Life-cycle assessment of carbon dioxide capture and utilization: avoiding the pitfalls," *Energy and Environmental Science*, vol. 6, pp. 2721-2734, 2013.
- [110] M. L. Godec, "CO<sub>2</sub>-EOR and CCUS: worldwide potential and commercial drivers," in *SPE Annual Technical Conference and Exhibition*, Amsterdam, The Netherlands, 2014.

- [111] OPIS, "Ethanol and biodiesel information service July 27, 2015," OPIS, 2015.
- [112] U.S. Grains Council, "Buying/Selling," U.S. Grains Council, 11 September 2015. [Online]. Available: <http://www.grains.org/buyingselling/ddgs>. [Accessed 22 September 2015].
- [113] J. Shi, Z. Li, Z. Cao, H. Wang, Y. Lu and Y. Wang, "Environmental impacts research for scroll compressor based on life cycle assessment," in International Conference on Materials, 2015.
- [114] M. Wang and H.-S. Huang, "A full fuel-cycle analysis of energy and emissions impacts of transportation fuels produced from natural gas," Argonne National Laboratory, 1999.
- [115] M. Goedkoop, R. Heijungs, M. Huijbregts, A. De Schryver, J. Struijs and R. van Zelm, "ReCiPe 2008 A life cycle impact assessment method which comprises harmonised category indicators at the midpoint and the endpoint level," *Ruimte en Milieu*, 2013.
- [116] P. Jaramillo, W. M. Griffin and S. T. McCoy, "Life cycle inventory of CO<sub>2</sub> in an enhanced oil recovery system," *Environmental Science and Technology*, vol. 43, no. 21, pp. 8027-8032, 2009.
- [117] M. Aresta and M. Galatola, "Life cycle analysis applied to the assessment of the environmental impact of alternative synthetic processes. The dimethylcarbonate case: part 1," *Journal of Cleaner Production*, vol. 7, pp. 181-193, 1999.
- [118] C. A. Trudewind, A. Schreiber and D. Haumann, "Photocatalytic methanol and methane production using captured CO<sub>2</sub> from coal-fired power plants. Part I - a life cycle assessment," *Journal of Cleaner Production*, vol. 70, pp. 27-37, 2014.

- [119] M. Wang, C. Saricks and M. Wu, "Fuel-cycle fossil energy use and greenhouse gas emissions of fuel ethanol produced from U.S. Midwest corn," Argonne National Laboratory, 1997.
- [120] I. Dincer and T. Ratlamwala, "Development of Novel Renewable Energy Based Hydrogen Production Systems: A Comparative Study," *Energy Conversion and Management*, vol. 72, pp. 77-87, August 2013.
- [121] G. A. Olah, A. Goepfert and G. K. Surya, "Chemical Recycling of Carbon Dioxide to Methanol and Dimethyl Ether: From Greenhouse Gas to Renewable, Environmentally Carbon Neutral Fuels and Synthetic Hydrocarbons," *The Journal of Organic Chemistry*, vol. 74, no. 2, pp. 487-498, 2009.